



저작자표시-비영리-변경금지 2.0 대한민국

이용자는 아래의 조건을 따르는 경우에 한하여 자유롭게

- 이 저작물을 복제, 배포, 전송, 전시, 공연 및 방송할 수 있습니다.

다음과 같은 조건을 따라야 합니다:



저작자표시. 귀하는 원저작자를 표시하여야 합니다.



비영리. 귀하는 이 저작물을 영리 목적으로 이용할 수 없습니다.



변경금지. 귀하는 이 저작물을 개작, 변형 또는 가공할 수 없습니다.

- 귀하는, 이 저작물의 재이용이나 배포의 경우, 이 저작물에 적용된 이용허락조건을 명확하게 나타내어야 합니다.
- 저작권자로부터 별도의 허가를 받으면 이러한 조건들은 적용되지 않습니다.

저작권법에 따른 이용자의 권리는 위의 내용에 의하여 영향을 받지 않습니다.

이것은 [이용허락규약\(Legal Code\)](#)을 이해하기 쉽게 요약한 것입니다.

[Disclaimer](#)

August 2023

Ph.D. Dissertation

**Biophysical and biological
characterization of host defense
peptides and hybrid conjugates by
peptide-membrane interaction
studies**

Graduate School of Chosun University

Department of Biomedical Sciences

Hyunhee Lee

**Biophysical and biological
characterization of host defense
peptides and hybrid conjugates
by peptide-membrane interaction
studies**

펩타이드와 세포막의 상호작용 연구를 통한

숙주방어 펩타이드와 하이브리드 접합체의 생물리

및 생물학적 특성 규명

2023년 8월 25일

Graduate School of Chosun University

Department of Biomedical Sciences

**Biophysical and biological
characterization of host defense
peptides and hybrid conjugates
by peptide-membrane interaction
studies**

Advisor: Prof. Song Yub Shin

*This dissertation is submitted to the Graduate School of
Chosun University in partial fulfillment of the requirements
for the degree of Doctor of Philosophy in Science*

April 2023

Graduate School of Chosun University

Department of Biomedical Sciences

Hyunhee Lee

Ph. D. Dissertation of

Hyunhee Lee is certified by

Chairman (Chosun Univ.): Prof. Seung Joo Cho

Committee Members

Chosun Univ. : Prof. Jung-Hee Lee

Chonnam Univ. : Prof. Chul Won Lee

Kwangju women's Univ. : Prof. Hye Jung Min

Chosun Univ. : Prof. Song Yub Shin

June 2023

Graduate School of Chosun University

CONTENTS

CONTENTS	i
LIST OF TABLES	iv
LIST OF FIGURES	v
ABSTRACT (KOREAN)	vi
ABSTRACT (ENGLISH)	x
PART I. Conjugation of cell-penetrating peptides with host defense peptides: A novel approach to combat drug-resistant bacteria	1
1. INTRODUCTION	2
2. MATERIALS AND METHODS	4
3. RESULTS	10
3.1. Effect of CPP-HDP conjugation on antimicrobial and hemolytic activities.....	10
3.2. Structural characterization.....	10
3.3. Membrane permeabilization and depolarization	11
3.4. LPS neutralization by peptides	13

3.5. The ability of CPP-HDP conjugates to translocation into liposomes..	14
3.6. Confocal laser-scanning microscopy.....	15
3.7. Interaction of the peptides with plasmid DNA.....	15
4. DISCUSSION	16
5. REFERENCES	27
PART II. Dimerization of host defense peptides: benefits and drawbacks for therapeutic applications	32
1. INTRODUCTION.....	33
2. MATERIALS AND METHODS.....	35
3. RESULTS	38
3.1. Circular dichroism (CD) studies.....	38
3.2. Antimicrobial and hemolytic activities of the peptides.....	38
3.3. Membrane permeabilization by peptides.....	39
3.4. Dye leakage form liposomes	39
3.5. The ability of peptides to translocation into liposomes.....	40
4. DISCUSSION	42

5. REFERENCES 50

PART III. Importance of structural arrangements of hydrophobic, amphipathic, and cationic domains in host defense peptides for antimicrobial activity 53

1. INTRODUCTION 54

2. MATERIALS AND METHODS 56

3. RESULTS 60

3.1. Peptide design and structure 60

3.2. Antimicrobial and hemolytic activity 60

3.3. Membrane depolarization and permeabilization 62

3.4. Binding of peptides to membranes by Trp fluorescence analysis 62

4. DISCUSSION 64

5. REFERENCES 76

LIST OF TABLES

PART I

Table 1. Amino acid sequences, molecular weights, and hemolytic activity of the HDPs and CPP-HDP conjugates used in this study.....	18
Table 2. Minimal inhibitory concentration (MIC) for the peptides against Gram-positive and Gram-negative bacteria.....	19

PART II

Table 1. Amino Acid Sequences and cytotoxic activities of peptides used in this study.....	44
Table 2. Antimicrobial activities of peptides against Gram-positive and Gram-negative bacteria	45
Table 3. Antimicrobial activities of peptides against antibiotic-resistant bacterial isolates	46

PART III

Table 1. Amino acid sequence, molecular weight, net charge, and hydrophobicity of the peptides used in this study	68
Table 2. Antimicrobial activities of peptides against Gram-positive and Gram-negative	69

LIST OF FIGURES

PART I

Figure 1. CD spectra of the peptides	20
Figure 2. Peptide-induced membrane permeabilization and depolarization .	21
Figure 3. LPS neutralization by the peptides.	23
Figure 4. Peptide translocation across lipid bilayers.	24
Figure 5. Confocal laser-scanning microscopy images of <i>E. coli</i> treated with FITC-labeled peptides	25
Figure 6. Peptide binding to DNA	26

PART II

Figure 1. CD spectra of the peptides	47
Figure 2. Ability of peptides to permeabilize membranes	48
Figure 1. Ability of peptides to translocate into liposomes.....	49

PART III

Figure 1. Structural isomers of amphipathic α -helical peptides.	70
Figure 2. CD spectra of the peptides	71
Figure 3. Dose-dependent curves of hemolytic activity	72
Figure 4. Killing kinetics of the peptides on bacterial cells	73
Figure 5. Membrane permeabilization caused by the peptides	74
Figure 6. Tryptophan fluorescence spectra and emission maxima (λ_{max}) for the peptides	75

초 록

펩타이드와 세포막의 상호작용 연구를 통한 숙주 방어 펩타이드와 하이브리드 접합체의 생물리 및 생물학적 특성 규명

이현희

지도교수: 신송엽 Ph.D.

의과학과,

조선대학교 대학원

PART I

수많은 병원체에 대한 선천적 면역의 필수 요소인 숙주방어 펩타이드(Host Defense Peptide, HDP)는 기존 항생제의 내성문제를 극복하기 위한 대안으로 큰 주목을 받아왔습니다. 본 연구에서는 HDP와 세포투과 펩타이드(Cell Penetrating Peptide, CPP)를 접합하여 항균활성을 향상시키는 새로운 접근 방법을 제안합니다. HDP-CPP 접합체는 그람 양성 박테리아에 대하여 접합하지 않은 HDP보다 2~4배 항균활성을 증가시켰고, 그람 음성 박테리아에 대한 항균활성은 4~16배 증가하는 결과를 나타내었습니다. HDP-CPP 접합체의 세포막 파괴 능력은 HDP와 유사하지만, 지질 이중층을 가로지르는 투과능력은 크게 향상 되었습니다. 형광 공초점 현미경을 사용하여

확인한 HDP의 분포는 주로 대장균의 세포막에 국한된 반면, HDP-CPP 접합체는 세균 세포막을 투과하여 세포 내부에 분포하였습니다. 또한, HDP-CPP 접합체는 HDP보다 DNA에 대해 더 높은 친화도를 나타내었습니다. 종합적으로, 본 연구는 HDP-CPP 접합체의 세포막 투과능력 및 DNA 결합능력을 포함한 다양한 기능적 특성이 그람 음성 박테리아에 대한 향상된 항균 활성과 연관이 있음을 보여줍니다. 따라서, HDP-CPP 접합은 그람 음성 박테리아에 대한 항균제의 개발을 위한 새로운 접근 방식이 될 수 있음을 제안합니다.

PART II

박테리아 막을 선택적으로 투과할 수 있는 숙주 방어 펩타이드(HDP)의 사용은 전통적인 항생제에 대한 유망한 대안 중 하나입니다. 본 연구에서는 세포막-표적 magainin II와 세포내부-표적 buforin II의 Lys으로 연결된 이량체를 만들었습니다. 이러한 이량체화는 펩타이드의 구조에 영향을 주지 않았지만, 항균 활성에는 큰 영향을 미쳤습니다. Magainin II 이량체는 항균 및 세포독성 효과를 증가시킨 반면, buforin II 이량체는 세포독성은 없으면서 항균 효능은 크게 증가시켰습니다. 흥미롭게도, buforin II 이량체는 항생제 내성 박테리아에 대한 항균 효과가 매우 뛰어났습니다. Magainin II 이량체는 음이온성 및

양쪽이온성 막을 둘 다 파괴시킨 반면, buforin II 이합체는 음이온성 막을 선택적으로 파괴한다는 것을 밝혔습니다. 또한, buforin II 이합체는 단량체 형태와 유사하게 지질 이중층을 가로질러 효율적으로 투과되었습니다. 이러한 결과는 buforin II를 이량체화 하는 것이 박테리아 막을 파괴할 뿐만 아니라 막을 가로질러 이동 가능하게 하여 세포내 구성 요소를 표적으로 삼아 효과적인 항균 활성을 나타낸다는 것을 시사합니다. 따라서 세포내 표적 HDP의 이량체화는 병원성 박테리아의 치료를 위한 우수한 전략이 될 수 있다고 제안합니다.

PART III

박테리아에 대한 숙주 방어 펩타이드(HDP)의 효능은 병원성 막과 상호 작용할 수 있는 HDP의 구조적 유연성에 의해 크게 영향을 받습니다. 양친매성 helix-hinge-helix 구조를 갖는 HDP는 연속적인 긴 나선형 HDP와 달리 숙주 세포에 대한 손상을 피하면서 강력한 항균 활성을 갖는 것으로 밝혀졌습니다. 그러나 양친매성 helix-hinge-helix 구조를 갖는 HDP의 구조와 활성간의 상관관계 및 살균 효과의 기본 메커니즘은 아직 완전히 이해되지 않았습니다. 이를 규명하기 위해 연속된 긴 α -helical peptide(KL)와 3개의 양친매성 helix-hinge-helix peptides(KL-KL, KL-L, KL-K)를 합성하여 이들의 생물학적, 구조적,

물리화학적 특성을 분석하였습니다. 양친매성 helix-hinge-helix 펩타이드의 항균 활성과 세포 독성은 다르지만, KL에 비해 항균 활성이 향상되었고 용혈 활성은 감소되었습니다. 양친매성 helix-hinge-helix 펩타이드 중 KL-K는 용혈효과는 없으면서 그람양성균과 그람음성균 모두에 대해 가장 강력한 항균 활성을 보였습니다. KL-L은 KL-K보다 세균 성장 효과는 낮았지만, 세균 막전위를 소멸시키면서 높은 살균 효과를 나타내었습니다. KL-K는 막을 크게 교란시키지 않고 지질 이중층을 통과하는 것으로 보여집니다. KL-KL은 KL-K와 KL-L 사이의 중간 구조적 및 기능적 특성을 나타내었습니다. 결론적으로 HDP의 구조적 배열이 막 투과성과 세포 침투 모두에 중요하며, 양친매성 helix-hinge-helix 구조를 갖는 HDP가 두 기능을 동시에 조절함으로써 항균제 개발에 유망한 방법이 될 수 있음을 시사합니다.

ABSTRACT

Biophysical and biological characterization of host defense peptides and hybrid conjugates by peptide-membrane interaction studies

Hyunhee Lee

Advisor: Prof. Song Yub Shin

Department of Biomedical sciences,

Graduate School of Chosun University

PART I

Host defense peptides (HDPs) are essential components of the innate immune system and have been explored as potential alternatives to traditional antibiotics. They function by disrupting the cell membrane of bacteria, leading to a broad-spectrum antimicrobial effect. In this study, a novel method was introduced to enhance the antimicrobial activity of HDPs by conjugating them with a cationic cell-penetrating peptide (CPP). Interestingly, the conjugated HDPs exhibited a significant increase in antimicrobial activity against Gram-negative bacteria (4-16 fold) compared to Gram-positive bacteria (2-4 fold). Although the conjugates did not increase membrane permeability, they effectively translocated across the lipid bilayer and penetrated the bacterial cells. Moreover, the conjugates showed a higher affinity for DNA than unconjugated HDPs. Collectively, the findings suggest

that CPP-HDP conjugates possess various functional properties that contribute to their enhanced antibiotic activity against Gram-negative bacteria, making them a promising candidate for the development of antimicrobial agents.

PART II

The use of host defense peptides (HDPs) that can selectively permeabilize bacterial membranes is a promising alternative to traditional antibiotics. However, the dimerization of HDPs is a strategy that has both potential benefits and drawbacks. Although it can enhance antimicrobial and membrane-lytic activity, it can also increase hemolytic and cytotoxic activity, which is undesirable. In this study, I created Lys-linked homodimers of magainin II and buforin II, which are membrane-permeabilizing and cell-penetrating peptides, respectively. While dimerization did not significantly affect the conformation of the peptides, it had a significant impact on their antimicrobial properties. I found that the magainin II dimer had increased antimicrobial and cytotoxic effects, while the buforin II dimer exhibited greater antibacterial potency without any cytotoxic activity. Interestingly, the buforin II dimer was highly effective against antibiotic-resistant bacterial isolates. My experiments on membrane permeabilization revealed that the magainin II dimer disrupted both anionic and zwitterionic membranes, whereas the buforin II dimer selectively disrupted anionic membranes. Moreover, the buforin II dimer was efficiently translocated across lipid

bilayers, similar to the monomeric form. My findings suggest that dimerization of cell-penetrating buforin II not only disrupts the bacterial membrane but also translocates it across the membrane to target intracellular components, resulting in effective antimicrobial activity. Hence, I propose that dimerization of intracellular targeting HDPs could be a superior strategy for therapeutic control of pathogenic bacteria.

PART III

The efficacy of host defense peptides (HDPs) against bacteria is strongly influenced by their structural flexibility and local backbone distortions that allow them to interact with pathogenic membranes. HDPs that exhibit a helix-hinge-helix structure with amphipathic properties have been found to have strong antibacterial activity while avoiding harm to host cells, unlike continuous long helical HDPs. However, the mechanism underlying the structure-activity relationship and bactericidal effect of helix-hinge-helix HDPs is not yet fully understood. To shed light on this, I synthesized a continuous long α -helical peptide (KL) and three helix-hinge-helix peptides (KL-KL, KL-L, and KL-K) and analyzed their biological, structural, and physicochemical properties. My findings revealed that although the antibacterial activity and cytotoxicity of the helix-hinge-helix peptides varied significantly, they displayed enhanced antibacterial activity and reduced hemolytic activity compared to KL. Among the helix-hinge-helix peptides,

KL-K exhibited the strongest antimicrobial activity against both gram-positive and gram-negative bacteria without any hemolytic effects. KL-L was capable of killing bacteria within 60 minutes of exposure, whereas KL-K was almost ineffective in bactericidal effect even after approximately 4 hours, although KL-L was less efficient at inhibiting bacterial growth than KL-K. I observed that KL-L rapidly and strongly dissipated the membrane potential, whereas KL-K did not. KL-K appears to traverse lipid bilayers without significantly perturbing the membrane. The results suggest that the membrane permeabilization and cell penetration of peptides are related to bactericidal and bacteriostatic activity, respectively. KL-L had a highly ordered α -helical structure in a membranous environment and even in an aqueous buffer due to self-association. KL-KL had intermediate structural and functional properties between KL-K and KL-L. In conclusion, my study suggests that the structural arrangement of HDPs is crucial for both membrane permeabilization and cell penetration, and that helix-hinge-helix HDPs could be a promising avenue for developing antibacterial agents by regulating both functions simultaneously.

PART I

Conjugation of cell-penetrating peptides with host defense peptides: A novel approach to combat drug-resistant bacteria

1. Introduction

Host defense peptides (HDPs) are essential components of the innate immune system, exhibiting a wide spectrum of activity against both Gram-positive and Gram-negative bacteria (1-3). HDPs have garnered significant attention as potential new host defenses due to the increased tolerance of microbes to conventional antibiotics (4-12). As HDPs are positively charged, they are initially drawn to negatively charged molecules on the surfaces of microorganisms, such as lipopolysaccharides (LPS) in Gram-negative bacteria and teichoic acids in Gram-positive bacteria. Although their exact mechanisms of action are not fully understood, it is generally accepted that HDPs disrupt the bacterial cell membrane by depolarization and/or permeabilization (13-20). Additionally, some HDPs are believed to cross the membrane without causing significant permeabilization, inhibiting various intracellular functions such as the synthesis of cell wall components, nucleic acids, and proteins (21-24).

Cationic cell-penetrating peptides (CPPs) are known for their ability to cross cell membranes and facilitate the uptake of various molecules (25, 26), which is why arginine-rich CPPs like R9 are widely used as delivery vectors (25, 27). In this study, I employed R9 to augment the antimicrobial activity of HDPs through a dual mechanism of action involving membrane disruption and intracellular targeting. Specifically, I conjugated R9 to two HDPs, magainin and M15 (Table 1), and assessed their antimicrobial activity and cytotoxicity by measuring the minimum inhibitory concentration (MIC) and hemolysis levels, respectively. To gain insight into the mechanisms of HDP and conjugate antimicrobial activity, I conducted membrane depolarization and permeabilization assays and visualized their site of action using confocal laser-scanning

microscopy. My findings reveal that compared to HDPs, CPP-HDP conjugates display significantly enhanced antimicrobial activity against Gram-negative bacteria, possibly due to membrane depolarization and secondary intracellular targeting. This study highlights CPP-HDP conjugation as a novel approach for designing highly effective agents against Gram-negative bacteria, and the multiple functions of CPP-HDP conjugates suggest a lower likelihood of microorganisms developing antibiotic resistance against them.

2. Materials and Methods

2.1 Materials

All peptides were synthesized using the standard Fmoc-based solid-phase method on Rink amide MBHA resin. N- α -Fmoc (fluoren-9-yl-methoxycarbonyl) amino acids with orthogonal side-chain-protecting groups were purchased from Novabiochem (Läufelfingen, Switzerland). The reagents and solvents (highest commercially available purity) for peptide synthesis were obtained from Applied Biosystems (Foster City, CA, USA). For the FITC-labeled peptides, the Fmoc- ϵ -Ahx-OH was added to the N-terminus of the protected peptide using standard coupling conditions and it was confirmed that FITC-labeled peptides exhibited similar antimicrobial activity to their respective unlabeled peptides. The purity of the synthesized peptides was confirmed by analytical RP-HPLC (above 98% pure). The correct molecular mass of the purified peptides was confirmed by MALDI-TOF-MS (Shimadzu, Japan). The phospholipids were purchased from Avanti Polar Lipids (Alabaster, AL, USA). A membrane potential-sensitive probe, 3,3'-dipropylthiobarbituric acid [DiSC3(5)], was obtained from Molecular Probes (Eugene, OR, USA). All other reagents were of analytical grade.

2.2 Circular dichroism (CD) spectroscopy

A Jasco J-715 CD spectrophotometer (Tokyo, Japan) was used to record the CD spectra of the peptides. Measurements were taken from 190 to 250 nm with a 0.1 nm step resolution, 50 nm/min speed, 0.5 s response time, and 1 nm bandwidth. The CD spectra of the peptides were obtained by averaging four scans in 10 mM sodium phosphate buffer (pH 7.2) or 30 mM SDS micelles at 25 °C.

2.3 Antimicrobial and hemolytic activities

The antimicrobial activity against Gram-positive and Gram-negative bacteria (2×10^6 CFU/mL) was assessed using the broth microdilution method, as detailed in a previous study (50). Eight bacterial strains, including four Gram-positive strains (*Bacillus subtilis* (KCTC 3068), *Staphylococcus epidermidis* (KCTC 1917), *Enterococcus faecalis* (KCTC 2011), and *Staphylococcus aureus* (KCTC 1621)) and four Gram-negative strains (*Escherichia coli* (KCTC 1682), *Pseudomonas aeruginosa* (KCTC 1637), *Proteus vulgaris* (KCTC 2433), and *Salmonella typhimurium* (KCTC 1926)), were obtained from the Korean Collection for Type Cultures (KCTC) at the Korea Research Institute of Bioscience and Biotechnology (Daejeon, Korea). Hemolytic activity was tested using human red blood cells (1×10^6 cells/mL), as previously described (50), with zero and one hundred percent hemolysis determined in PBS and 0.1% Triton X-100, respectively.

2.4 Inner and outer membrane permeability

To assess the ability of the peptides to permeabilize the inner membrane, N-phenyl-1-naphthylamine (NPN) uptake into the outer membrane of *E. coli* (KCTC 1682) was measured, as previously described (51). *E. coli* cells were suspended in 5 mM HEPES buffer (pH 7.2) containing 5 mM KCN and the NPN dye was added to a final concentration of 10 μ M. Background fluorescence was recorded at 420 nm (excitation at 350 nm) using an RF-5301PC spectrofluorophotometer (Shimadzu, Japan). The peptides were added to the cuvette and the fluorescence was monitored until no further increase in fluorescence was observed. The increase in NPN fluorescence, which reflects increased outer membrane permeability, was quantified as % NPN uptake using

the formula: % NPN uptake = $(F_{obs}-F_0)/(F_{100}-F_0) \times 100$, where F_{obs} is the observed fluorescence at a given peptide concentration, F_0 is the initial fluorescence of NPN with *E. coli* cells in the absence of peptide, and F_{100} is the fluorescence of NPN with *E. coli* cells following addition of 10 $\mu\text{g/ml}$ polymyxin B. Inner membrane permeabilizing ability was determined by measuring β -galactosidase activity in *E. coli* ML-35 cells using the chromogenic substrate o-nitrophenyl- β -D-galactoside (ONPG), which is normally impermeable (52). The cells were washed in 10 mM sodium phosphate buffer (pH 7.2) containing 100 mM NaCl and resuspended in the same buffer containing 1.5 mM ONPG at a final concentration of OD600 = 0.5. The hydrolysis of ONPG to o-nitrophenol over time was monitored at 405 nm following addition of the peptides.

2.5 Membrane depolarization and disruption

To detect membrane depolarization, the membrane potential-sensitive probe DiSC3(5) was used, following a previously described method (53). *S. aureus* and *E. coli* were grown to mid-logarithmic phase in LB, then washed with HEPES buffer containing glucose (5 mM HEPES, 20 mM glucose, 100 mM KCl, pH 7.2) and resuspended in the same buffer to an OD600 of 0.05. Using the RF-5301 spectrofluorometer (Shimadzu), the fluorescence changes resulting from the collapse of the cytoplasmic membrane potential were monitored at excitation and emission wavelengths of 622 and 670 nm, respectively. Peptides were added to the cells once the fluorescence intensity had stabilized due to maximal dye uptake by the bacterial membranes, and gramicidin D (0.25 nM) was used to completely collapse the membrane potential. For membrane disruption determination, calcein release from large unilamellar vesicles (LUVs) was measured, as previously described (53). The fluorescence intensity of the calcein released from the

liposomes was monitored at 520 nm (excitation at 490 nm) using a Jasco FP-750 spectrofluorometer (Tokyo, Japan), and complete dye release was obtained using 0.1% Triton X-100.

2.6 LPS-neutralizing activity

To assess the ability of the peptides to inhibit or neutralize LPS, a Limulus amoebocyte lysate (LAL) assay kit (Kinetic-QCL 1000; BioWhittaker Inc., Walkersville, MD, USA) was used according to the manufacturer's instructions. In Gram-negative bacteria, LPS activates a proenzyme in LAL that catalyzes the release of a colored product, paranitroanilide (pNA), from the Ac-Ile-Glu-Ala-Arg-pNA substrate, which is detected spectrophotometrically at OD410. The peptides were dissolved in the pyrogen-free water supplied with the kit, and their pH was adjusted to 7.0 with 1 M HCl or 1 M NaOH prepared in pyrogen-free water. Increasing concentrations of the peptides were incubated with 1 endotoxin unit (EU) in a total volume of 50 μ l for 30 min at 37 °C. The peptide-EU complex was then mixed with approximately 50 μ l of LAL reagent, incubated for 10 min, and 100 μ l of substrate was added. After incubating the reaction for 6 min, the release of the colored product was recorded at OD410. Water served as a negative control (blank) instead of peptides, and it was considered as 0% inhibition. The percent LPS neutralization was calculated using the formula % LPS neutralization = $[(OD_{\text{blank}} - OD_{\text{peptide}})/OD_{\text{blank}}] \times 100$.

2.7 Peptide translocation

To evaluate the ability of HDPs and CPP-HDP conjugates to cross a phospholipid membrane, a fluorescence transfer assay was conducted, as previously described (54). In brief, unilamellar liposomes consisting of

POPC/POPG/DNS-PE (50:45:5) and 200 μ M chymotrypsin in buffer (20 mM HEPES, 150 mM NaCl, pH 7.2) were prepared by extrusion. The suspension was then treated with a trypsin-chymotrypsin inhibitor to inactivate all extraliposomal enzymes. The peptides (2 μ M) were added to the suspension, and fluorescence transfer from the peptides' Trp residues to the DNS-PE dansyl group was monitored using a Shimadzu RF 5301 PC spectrofluorometer. Excitation of Trp residues at 280 nm resulted in fluorescence transfer to the DNS-PE dansyl group, with emission measured at 510 nm. Decreased fluorescence following peptide addition indicated degradation of the internalized peptide by the liposomal enzyme. The measurements were repeated three times.

2.8 Confocal laser-scanning microscopy

The *Escherichia coli* (KCTC 1682) cells were cultured until the midlogarithmic phase, followed by centrifugation and washing with 10 mM phosphate buffer saline (pH 7.2) thrice. The bacterial cells (1×10^7 CFU/ml) were then incubated with FITC-labeled peptides (0.2 μ M) at 37°C for 30 min. The cells were washed with 10 mM sodium phosphate buffer and then fixed onto a glass slide. The FITC-labeled peptides were visualized using an Olympus IX 70 confocal laser-scanning microscope (Tokyo, Japan), with fluorescent images acquired using a 488-nm band-pass filter for FITC excitation.

2.9 DNA binding assay

To select the closed, circular form of the plasmid, plasmid DNA was purified using CsCl density-gradient ultracentrifugation. Gel retardation experiments were conducted by incubating 300 ng of the plasmid DNA (pBluescript II SK+) with increasing peptide concentrations in 20 μ l of binding

buffer (5% glycerol, 10 mM Tris-HCl pH 8.0, 1 mM EDTA, 1 mM dithiothreitol, 20 mM KCl, and 50 μ g/ml bovine serum albumin) at room temperature for 1 h. Following this, 4 μ l of native loading buffer (10% Ficoll 400, 10 mM Tris-HCl pH 7.5, 50 mM EDTA, 0.25% bromophenol blue, and 0.25% xylene cyanol) was added and a 20 μ l aliquot was electrophoresed in a 1% agarose gel in 0.5 \times Tris borate-EDTA buffer (45 mM Tris-borate and 1 mM EDTA, pH 8.0). Ethidium bromide fluorescence was used to detect the migration of DNA.

3. Results

3.1 Effect of CPP-HDP conjugation on antibacterial and hemolytic activities

The peptides used in this study, magainin and M15, are cationic and amphipathic α -helical peptides that are thought to work by permeabilizing cytoplasmic membranes. R9 is an arginine-rich CPP that can cross cell membranes. To test their cytotoxicity and ability to kill bacteria, both the HDPs (magainin and M15) and the CPP-conjugated HDPs (R9-magainin and R9-M15) were evaluated using human erythrocytes (Table 1) and bacteria (Table 2). Magainin and M15 showed low hemolytic activity and moderate antibacterial activity against all tested Gram-positive and -negative bacteria, with MIC values ranging from 8 to 32 μ M. Conjugation with R9 did not increase cytotoxicity, and only slightly improved antibacterial activity against Gram-positive bacteria. However, the CPP-HDP conjugates showed a significant improvement in antimicrobial activity (4-16 fold) against Gram-negative bacteria, with MIC values in the 1 to 4 μ M range. R9 alone did not have any antimicrobial activity, even at a concentration of 128 M. The presence of R9 had limited effect on the MICs of magainin and M15 at a concentration of 16 M. These findings suggest that CPP conjugation to HDPs can greatly enhance their antimicrobial activity, particularly against Gram-negative bacteria.

3.2 Structural characterization

To further investigate, I utilized circular dichroism (CD) spectroscopy to examine the secondary structure of magainin, M15, and their R9 conjugates (R9-magainin and R9-M15) in both aqueous buffer and membrane-mimicking

environments (Fig. 1). In aqueous buffer, all peptides showed negative bands at around 200 nm, suggesting that their structures were random. However, when exposed to 30 mM SDS micelles, the peptides displayed two negative bands at 208 nm and 222 nm and a positive band at 195 nm, indicating that they adopt an α -helical structure in membrane environments. Although the R9 conjugates exhibited a relatively strong negative band at 205 nm, indicating a structure somewhat different from a typical α -helix, likely due to the flexible R9 sequences, the overall CD spectral patterns were similar between HDPs and CPP-HDP conjugates, indicating that CPP conjugation did not significantly affect the amphipathic α -helical structure of the HDPs.

3.3 Membrane permeabilization and depolarization

To determine how much of the peptides' antimicrobial activity was due to their ability to permeabilize the membrane of Gram-negative bacteria, the researchers investigated the ability of the peptides to increase the permeability of the outer and inner membranes of *E. coli*. They used the fluorescent probe NPN to measure the uptake of the probe into the outer membrane of *E. coli*, which would indicate membrane destabilization. They found that both the HDPs and CPP-HDP conjugates induced NPN uptake in a dose-dependent manner, suggesting that they can disrupt the outer membrane barrier. However, there was no significant difference in the permeabilizing activity between the two groups, so the enhanced antimicrobial activity of the CPP-HDP conjugates could not be explained by this. The researchers then investigated the ability of the peptides to permeabilize the inner membrane of *E. coli*, using cells lacking the lactose permease enzyme. They found that all the peptides induced inner membrane permeability in a concentration-dependent manner, but there were only marginal differences in the

degrees of inner membrane permeabilization between the HDPs and CPP-conjugated HDPs. This suggests that the permeabilization of the inner membrane is not related to the increased antimicrobial potency of the conjugates.

As Gram-negative bacteria showed greater sensitivity to CPP-HDP conjugates, I examined membrane depolarization in *Staphylococcus aureus* and *Escherichia coli*, representative of Gram-positive and Gram-negative bacteria, respectively (as shown in Figure 2C). I used the fluorescent dye DiSC3(5) to evaluate the peptides' ability to depolarize the membrane. This dye integrates into the cytoplasmic membrane, and its fluorescence is impacted by the membrane potential gradient. Magainin and M15 depolarized the cytoplasmic membrane of both *S. aureus* and *E. coli* below their MIC values, as expected. However, the CPP-HDP conjugates also induced effective membrane depolarization, similar to that of the unconjugated HDPs. Consequently, there was no direct correlation between cytoplasmic membrane depolarization and MIC values, suggesting that other mechanisms likely contribute to the potent antimicrobial activity of CPP-conjugated HDPs against Gram-negative bacteria.

To investigate the peptides' ability to cause membrane permeabilization, I conducted experiments using negatively charged PC/PG (1:1) and zwitterionic PC liposomes (Fig. 2D) and measured the release of entrapped calcein into the buffer after adding the peptides to the liposomes, which causes lysis. The results showed that all the peptides had a weak ability to disrupt zwitterionic PC liposomes, which was consistent with the hemolytic activity findings. In negatively charged liposomes, both HDPs and CPP-conjugated HDPs showed strong membrane-lytic activity, which was in line with their respective abilities to depolarize bacterial cell membranes. However, this similarity in membrane-lytic activity does not

explain the increased antimicrobial activity of the CPP-HDP conjugates. Although membrane disruption is a significant bactericidal mechanism for HDPs, the potent antimicrobial effect of CPP-conjugated HDPs against Gram-negative bacteria likely involves other targets.

3.4 LPS neutralization by peptides

HDPs are known to initially interact with LPS on the surface of Gram-negative bacteria, and the permeability of the outer membrane is an important factor in their antimicrobial activity (28). Some HDPs have been shown to bind to LPS and neutralize it, leading to effective bactericidal and anti-inflammatory activities against Gram-negative bacteria (29, 30). In order to investigate whether the enhanced antimicrobial activity of CPP-HDP conjugates is associated with their ability to bind to LPS, the researchers used a *Limulus* amoebocyte lysate (LAL) assay to measure their LPS neutralization capacity (Fig. 3A). All the peptides were found to neutralize LPS activity in a dose-dependent manner, and the CPP-HDP conjugates showed stronger LPS-neutralizing activity than the unconjugated HDPs. These findings suggest that the increased LPS-neutralizing activity of CPP-conjugated HDPs may be linked to their antimicrobial activity against Gram-negative bacteria.

To trigger cytokine production, LPS activates inflammatory pathways (31). To further explore the peptides' ability to neutralize LPS, I evaluated their impact on LPS-induced tumor necrosis factor-alpha (TNF- α) release and nitric oxide (NO) production in RAW264.7 macrophage cells (Fig. 3B). Treatment of the cells with 20 ng/ml LPS resulted in the release of TNF- α and NO. In comparison to magainin and M15 alone, the R9 conjugates (R9-magainin and R9-M15) considerably suppressed TNF- α release and NO production in LPS-

stimulated RAW264.7 cells, indicating that the conjugates bind to LPS more effectively than unconjugated HDPs. The efficient binding of CPP-HDP conjugates to LPS may partly explain their superior antimicrobial activity against Gram-negative bacteria. These findings also suggest that CPP conjugation to HDPs is a promising strategy for developing anti-inflammatory agents.

3.5 The ability of CPP-HDP conjugates to translocate into liposomes

Recently, studies have found that some peptides exhibit strong bactericidal activity without causing significant membrane permeabilization (21, 23, 32, 33). These peptides are believed to kill bacteria by interfering with DNA or protein synthesis. Since the antimicrobial activity of HDPs may be linked to intracellular targets, the researchers investigated whether the peptides could translocate across membranes. They used a method involving resonance energy transfer from the Trp residues of the peptides to the dansyl group of DNS-PE in the membrane to monitor the peptides' translocation across PC/PG (1:1) liposomes (Fig. 4). They observed the degradation of the peptides by chymotrypsin, which was confined in the liposomes. Fluorescence intensity increased when the peptide solution (2 μM) was added to liposomes (200 μM), indicating binding of the peptide to the membrane via resonance energy transfer from the Trp residue to DNS-PE. After translocation, chymotrypsin should digest the peptide, resulting in reduced fluorescence intensity. Magainin and M15 showed only a small change in fluorescence, indicating a lack of membrane translocation. However, R9-magainin and R9-M15 both caused a time-dependent reduction in fluorescence intensity, indicating that the peptides efficiently translocated across the lipid bilayer.

3.6 Confocal laser-scanning microscopy

In order to investigate the penetration of CPP-HDP conjugates into bacterial cells, I treated *E. coli* with FITC-labeled peptides and observed their localization using confocal laser-scanning microscopy (Fig. 5). As anticipated, FITC-labeled magainin was found to be bound to the surface of *E. coli* cells, indicating that its primary site of action is the bacterial membrane. In contrast, FITC-labeled R9-magainin penetrated the membranes and accumulated in the cytoplasm of *E. coli*. These findings suggest that CPP-conjugated HDPs have a secondary target inside the cell.

3.7 Interaction of the peptides with plasmid DNA

To explore the peptides' potential to target intracellular molecules after penetrating cell membranes, I investigated their DNA-binding properties. I used plasmid DNA migration retardation assay to evaluate peptide interactions with DNA (Fig. 6). Different peptide concentrations were incubated with 200 ng of plasmid DNA at room temperature for 30 minutes, and the reaction mixtures were analyzed on a 1% agarose gel. Magainin did not significantly affect DNA migration, even at concentrations up to 128 $\mu\text{g/ml}$. Conversely, R9-magainin completely inhibited DNA migration at a concentration of 2 $\mu\text{g/ml}$, indicating its efficient binding to DNA.

4. Discussion

Host defense peptides have been extensively studied as a novel class of antibiotics due to their rapid and broad-spectrum antimicrobial activities and reduced likelihood of eliciting microbial resistance (34, 35). The mechanism by which HDPs exert their antimicrobial activity is generally accepted to be through bacterial membrane depolarization and permeabilization (36-39). However, there is often no correlation between the degree of permeabilization associated with several HDPs and their antimicrobial activity (40-42). Recent studies have shown that some antibacterial peptides have bactericidal effects involving multiple modes of action, including membrane disruption coupled with secondary intracellular targeting (43, 44). My study demonstrated that the introduction of CPP and HDP simultaneously did not contribute to antimicrobial activity, as there was no observed synergistic effect. However, CPP conjugation to HDPs led to improved antimicrobial activity against Gram-negative bacteria without cytotoxicity. Although the CPP-HDP conjugates were able to depolarize and permeabilize bacterial cell membranes and model liposomes, their capacity was not different from that observed for HDPs alone. However, CPP conjugation to HDPs facilitated their translocation across the membrane and entry into bacterial cells. The DNA retardation assay revealed that CPP-HDP conjugates had a higher affinity for DNA than the HDPs alone. The high positive charge of the conjugated peptide allowed for interaction with negatively charged molecules in cells. Therefore, the increased antimicrobial activity observed for the CPP-conjugated HDPs could be explained by membrane disruption coupled with secondary intracellular targeting.

There is a growing threat to public health due to the development of

resistance in numerous bacteria against existing antibiotics (45, 46). Of particular concern are Gram-negative bacteria which possess a protective outer membrane composed of LPS (47, 48). The initial step in the interaction between bacterial membranes and HDPs is believed to be the binding of positively charged peptides to negatively charged LPS on the bacterial surface. Due to the permeability barrier function of the outer membrane, Gram-negative bacteria are protected from the lytic activity of some antimicrobial proteases (49), making the overcoming of the outer membrane permeability barrier a prerequisite for the effectiveness of antimicrobial agents. The conjugates were found to exhibit enhanced anti-inflammatory activity compared to HDPs alone in LPS-stimulated macrophages, likely through the neutralization of LPS. The binding to LPS may also facilitate conjugate delivery to its site of action, thus increasing antimicrobial activity against Gram-negative bacteria. Furthermore, these findings suggest that CPP conjugation to HDPs may be an effective strategy for developing anti-inflammatory agents.

As far as I know, no previous studies have investigated the effects of CPP-HDP conjugates on antimicrobial activity and their mechanism of action. My findings indicate that CPP conjugation to HDPs could be a promising approach for improving antimicrobial activity and selectivity against Gram-negative bacteria. Additionally, my results suggest that CPP conjugation can confer several additional functions on HDPs, including LPS-binding, transmembrane translocation, and DNA binding, which are critical for enhanced antimicrobial activity. Thus, my CPP-HDP conjugation design may represent a potential strategy for developing new antimicrobial drugs to combat multidrug-resistant bacteria.

Table 1 Amino acid sequences, molecular weights, and hemolytic activity of the HDPs and CPP-HDP conjugates used in this study.

Peptides	Amino acid sequences	Mass		Hemolysis
		Calculate d	Observed	
Magainin	GIGKWLHSAKKFGKAFVGEIMNS	2505.9	2506.7	2.8%
R9-magainin	RRRRRRRRRGGGGIGKWLHSAKKFGKAFVGEIMNS	4082.8	4083.4	2.3%
M15	KWKLLKLLKLLKK	1908.5	1909.2	6.1%
R9-M15	RRRRRRRRRGGGKWKLLKPLKLLKK	3469.3	3469.9	6.7%

Table 2. Minimal inhibitory concentration (MIC) for the peptides against Gram-positive and Gram-negative bacteria.

Organism	antimicrobial activity (MIC: μM)			
	Magainin (-R9 / +R9) ^a	R9-magainin	M15 (-R9 / +R9) ^a	R9-M15
Gram-positive bacteria				
<i>B. subtilis</i>	8 / 8	2-4	8-16 / 8-16	4-8
<i>S. aureus</i>	16-32 / 16	8	8 / 8	4
<i>E. faecalis</i>	16 / 16	4	16 / 8	4-8
<i>S. epidermidis</i>	16 / 8-16	4-8	16-32 / 16	8
Gram-negative bacteria				
<i>E. coli</i>	32 / 32	2-4	16-32 / 16	2-4
<i>S. typhimurium</i>	16-32 / 16-32	1-2	32 / 32	2
<i>P. aeruginosa</i>	32 / 32	4	32 / 32	4
<i>P. vulgaris</i>	32-64 / 32	4-8	32 / 32	4-8

^aantimicrobial activity tested in the presence (+R9) or absence (-R9) of 16 μM R9. Alone, R9 did not exhibit antimicrobial activity, even at the highest tested concentration of 128 μM

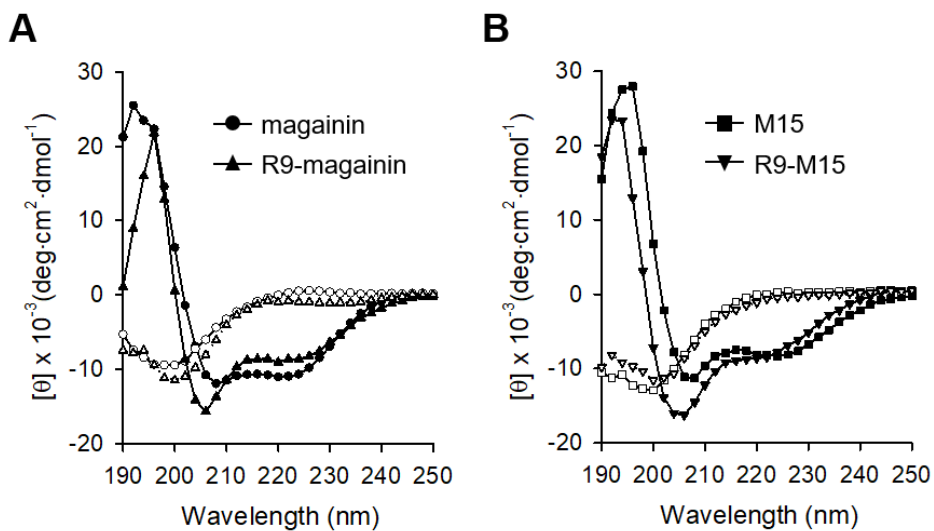


Fig. 1. CD spectra of the peptides. The CD spectra of magainin and R9-magainin (A) and M15 and R9-M15 (B) were obtained at 25 °C in aqueous buffer (open symbols), or 30 mM SDS micelles (closed symbols) in the presence of 25 μM concentrations of magainin (○), R9-magainin (△), M15 (□), and R9-M15 (▽).

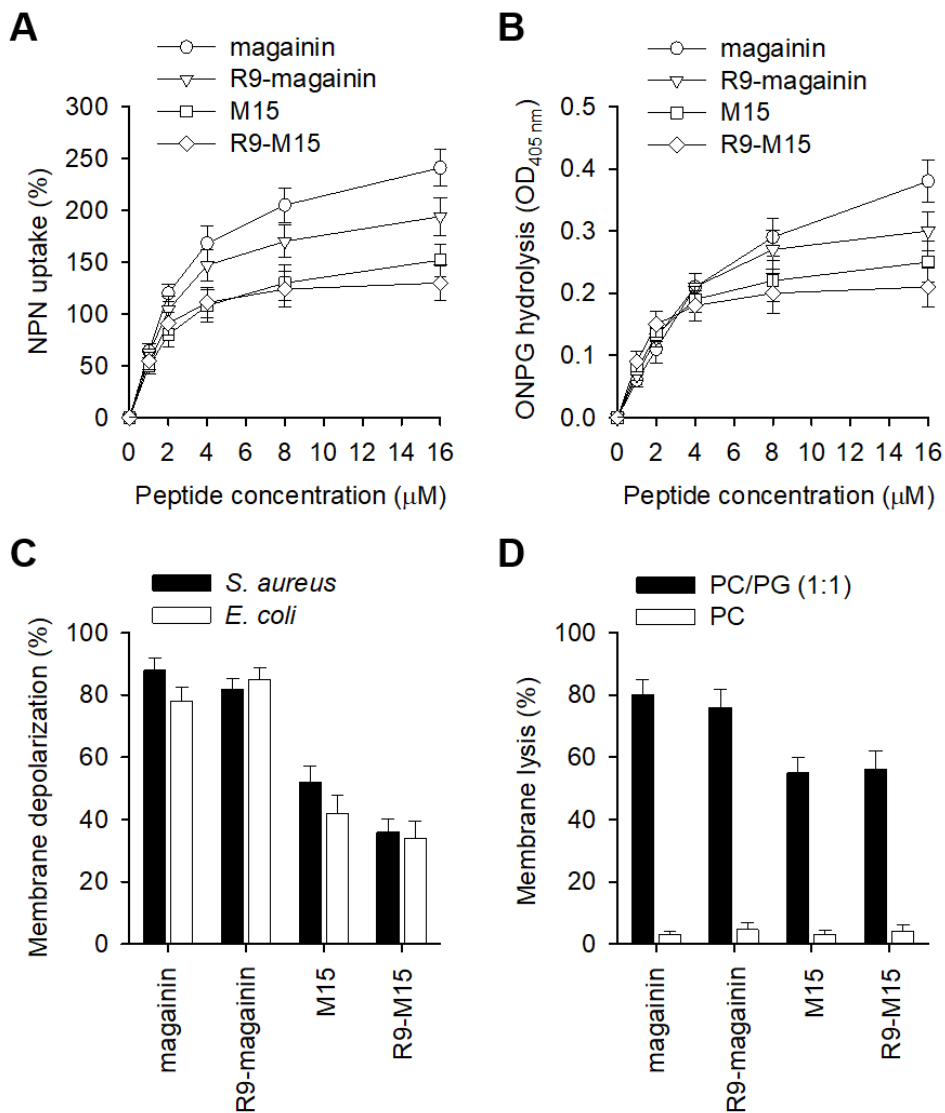


Fig. 2. Peptide-induced membrane permeabilization and depolarization. (A) Outer membrane permeability of *E. coli* induced by the peptides. *E. coli* were incubated with NPN in the presence of various concentrations of the peptides. The NPN uptake was determined by a fluorescence increase resulting from the NPN partitions into the

hydrophobic interior of the outer membrane. (B) Permeabilization of the inner membrane of *E. coli* ML-35 cells by the peptides. Permeabilization was determined by the unmasking of cytoplasmic β -galactosidase, as assessed by hydrolysis of the impermeable, chromogenic substrate ONPG. (C) Membrane depolarization of intact *S. aureus* and *E. coli* cells by the peptides. The peptides were added after the fluorescence of membrane potential-sensitive dye DiSC3(5) was stabilized. In order for DiSC3(5) to reach the cytoplasmic membrane of Gram-negative bacteria, *E. coli* were pretreated with EDTA (15 mM). (D) Membrane permeabilization of negatively charged PC/PG (1:1) or neutral PC liposomes by the peptides visualized with the fluorescent dye calcein. The peptides (2 μ M) were added into 100 μ M liposomes. The error bars represent standard deviations of the mean determined from three independent experiments.

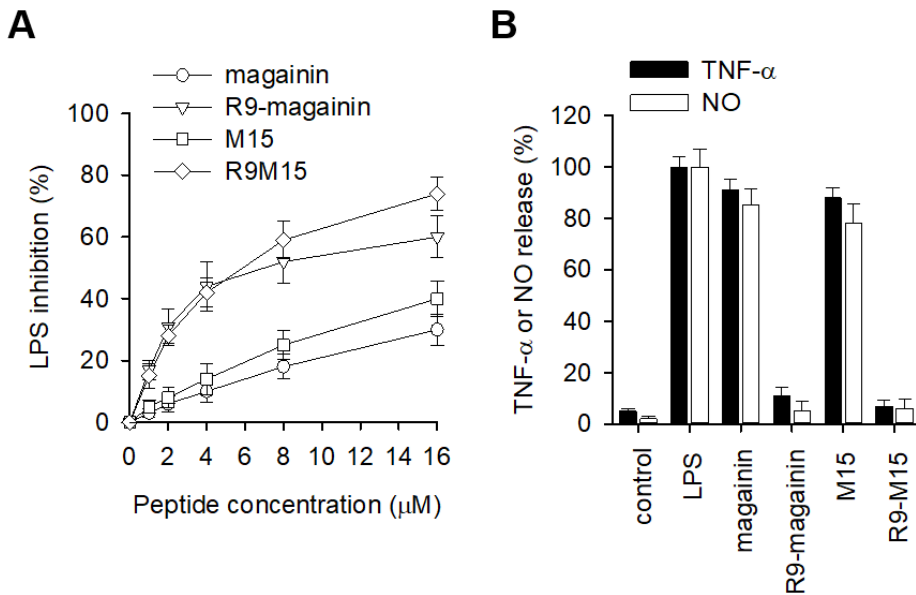


Fig. 3. LPS neutralization by the peptides. (A) The LPS-neutralizing activity of the peptides as determined by the LAL assay. LPS was incubated with different peptide concentrations for 30 min. (B) Inhibitory effect of peptides on TNF- α release and NO production from LPS-stimulated RAW264.7 cells. The cells (5×10^5 cells/ml) were treated with 20 ng/ml LPS in the presence or absence of 2 μ M of each peptide. The error bars represent standard deviations of the mean determined from three independent experiments.

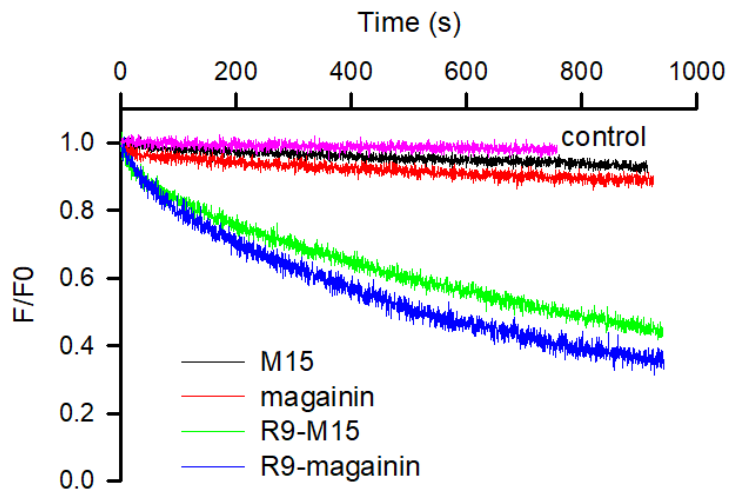


Fig. 4. Peptide translocation across lipid bilayers. Peptide translocation across the membrane was monitored by measuring the resonance energy transfer from the Trp residues of the peptides to the dansyl group of DNS-PE incorporated into the liposomes. Once peptides are translocated into liposomes, the internalized peptides are degraded by α -chymotrypsin trapped in the liposome, which eventually reduces fluorescence. The peptide and lipid concentrations were 2 and 200 μ M, respectively.

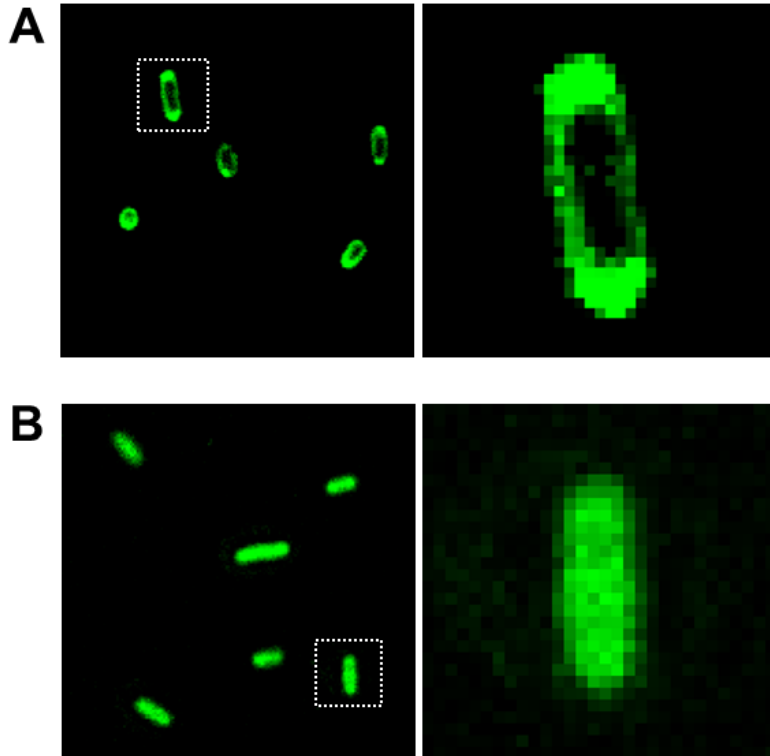


Fig. 5. Localization of the peptides in *E. coli* cells. *E. coli* were incubated with FITC-labeled magainin (A) or FITC-labeled R9-magainin conjugate (B) for 30 min at 37 °C and imaged by confocal laser-scanning microscopy.

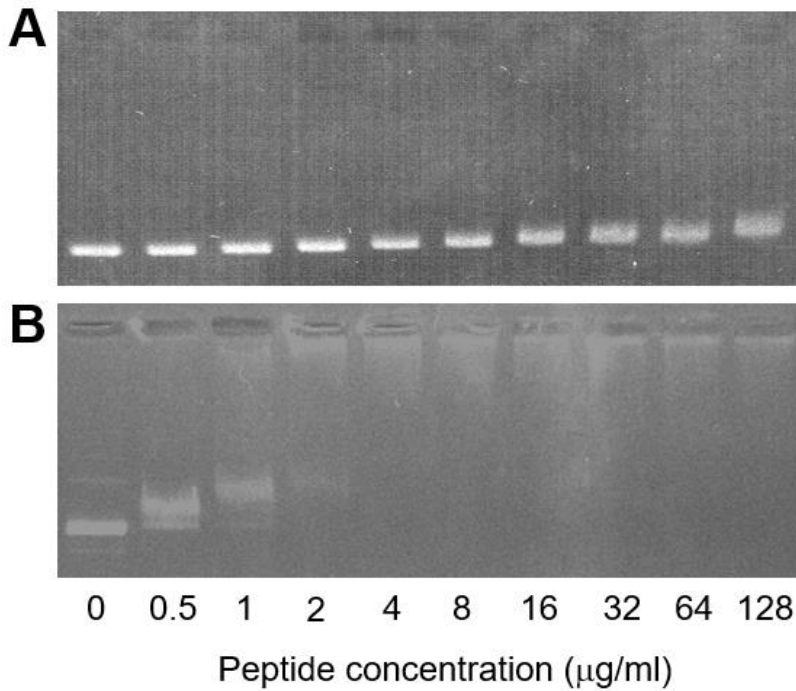


Fig. 6. Peptide binding to DNA. The interaction of magainin (A) and R9-magainin (B) with plasmid DNA was assessed by measuring the retardation of plasmid DNA migration through a 1% agarose gel. The peptide concentration indicated in each lane represents a serial increase in concentration from 0.5 to 128 $\mu\text{g/ml}$

References

1. E. F. Haney, S. K. Straus, R. E. W. Hancock, Reassessing the Host Defense Peptide Landscape. *Front Chem* **7**, 43 (2019).
2. A. L. Hilchie, K. Wuerth, R. E. Hancock, Immune modulation by multifaceted cationic host defense (antimicrobial) peptides. *Nat Chem Biol* **9**, 761 (Dec, 2013).
3. L. J. Zhang, R. L. Gallo, Antimicrobial peptides. *Curr Biol* **26**, R14 (Jan 11, 2016).
4. Z. Y. Yang *et al.*, Rational Design of Short Peptide Variants by Using Kunitzin-RE, an Amphibian-Derived Bioactivity Peptide, for Acquired Potent Broad-Spectrum Antimicrobial and Improved Therapeutic Potential of Commensalism Coinfection of Pathogens. *J Med Chem* **62**, 4586 (May 9, 2019).
5. D. Faccone *et al.*, Antimicrobial activity of de novo designed cationic peptides against multi-resistant clinical isolates. *Eur J Med Chem* **71**, 31 (Jan, 2014).
6. Z. Ma *et al.*, Insights into the Antimicrobial Activity and Cytotoxicity of Engineered alpha-Helical Peptide Amphiphiles. *J Med Chem* **59**, 10946 (Dec 22, 2016).
7. R. I. Lehrer, A. M. Cole, M. E. Selsted, theta-Defensins: cyclic peptides with endless potential. *J Biol Chem* **287**, 27014 (Aug 03, 2012).
8. N. K. Brogden, K. A. Brogden, Will new generations of modified antimicrobial peptides improve their potential as pharmaceuticals? *Int J Antimicrob Agents* **38**, 217 (Sep, 2011).
9. K. Lohner, Membrane-active Antimicrobial Peptides as Template Structures for Novel Antibiotic Agents. *Curr Top Med Chem*, (Jul 13, 2016).
10. M. Mahlapuu, J. Hakansson, L. Ringstad, C. Bjorn, Antimicrobial Peptides: An Emerging Category of Therapeutic Agents. *Front Cell Infect Microbiol* **6**, 194 (2016).
11. L. S. Biswano, M. G. da Costa Sousa, T. M. B. Rezende, S. C. Dias, O. L. Franco, Antimicrobial Peptides and Nanotechnology, Recent Advances and Challenges. *Front Microbiol* **9**, 855 (2018).
12. A. de Breij *et al.*, The antimicrobial peptide SAAP-148 combats drug-resistant

- bacteria and biofilms. *Sci Transl Med* **10**, (Jan 10, 2018).
13. T. A. Stone *et al.*, Positive Charge Patterning and Hydrophobicity of Membrane-Active Antimicrobial Peptides as Determinants of Activity, Toxicity, and Pharmacokinetic Stability. *J Med Chem*, (Jul 1, 2019).
 14. S. Guha, J. Ghimire, E. Wu, W. C. Wimley, Mechanistic Landscape of Membrane-Permeabilizing Peptides. *Chem Rev*, (Jan 9, 2019).
 15. Y. Lyu *et al.*, Design of Trp-rich dodecapeptides with broad-spectrum antimicrobial potency and membrane-disruptive mechanism. *J Med Chem*, (Jul 5, 2019).
 16. L. T. Nguyen, E. F. Haney, H. J. Vogel, The expanding scope of antimicrobial peptide structures and their modes of action. *Trends Biotechnol* **29**, 464 (Sep, 2011).
 17. Y. Shai, Mode of action of membrane active antimicrobial peptides. *Biopolymers* **66**, 236 (2002).
 18. M. A. Sani, F. Separovic, How Membrane-Active Peptides Get into Lipid Membranes. *Acc Chem Res* **49**, 1130 (Jun 21, 2016).
 19. P. Kumar, J. N. Kizhakkedathu, S. K. Straus, Antimicrobial Peptides: Diversity, Mechanism of Action and Strategies to Improve the Activity and Biocompatibility In Vivo. *Biomolecules* **8**, (Jan 19, 2018).
 20. K. Matsuzaki, Control of cell selectivity of antimicrobial peptides. *Biochim Biophys Acta* **1788**, 1687 (Aug, 2009).
 21. P. Nicolas, Multifunctional host defense peptides: intracellular-targeting antimicrobial peptides. *FEBS J* **276**, 6483 (Nov, 2009).
 22. F. Guilhelmelli *et al.*, Antibiotic development challenges: the various mechanisms of action of antimicrobial peptides and of bacterial resistance. *Front Microbiol* **4**, 353 (Dec 09, 2013).
 23. S. T. Yang *et al.*, Possible role of a PXXP central hinge in the antibacterial activity and membrane interaction of PMAP-23, a member of cathelicidin family. *Biochemistry-US* **45**, 1775 (Feb 14, 2006).
 24. C. F. Le, C. M. Fang, S. D. Sekaran, Intracellular Targeting Mechanisms by Antimicrobial Peptides. *Antimicrob Agents Chemother* **61**, (Apr, 2017).
 25. N. Schmidt, A. Mishra, G. H. Lai, G. C. Wong, Arginine-rich cell-penetrating

- peptides. *FEBS Lett* **584**, 1806 (May 03, 2010).
26. F. Madani, S. Lindberg, U. Langel, S. Futaki, A. Graslund, Mechanisms of cellular uptake of cell-penetrating peptides. *J Biophys* **2011**, 414729 (2011).
 27. S. Futaki *et al.*, Arginine-rich peptides. An abundant source of membrane-permeable peptides having potential as carriers for intracellular protein delivery. *J Biol Chem* **276**, 5836 (Feb 23, 2001).
 28. Y. Rosenfeld, Y. Shai, Lipopolysaccharide (Endotoxin)-host defense antibacterial peptides interactions: role in bacterial resistance and prevention of sepsis. *Biochim Biophys Acta* **1758**, 1513 (Sep, 2006).
 29. Y. Sun, D. Shang, Inhibitory Effects of Antimicrobial Peptides on Lipopolysaccharide-Induced Inflammation. *Mediators Inflamm* **2015**, 167572 (2015).
 30. A. Giuliani, G. Pirri, A. C. Rinaldi, Antimicrobial peptides: the LPS connection. *Methods Mol Biol* **618**, 137 (2010).
 31. R. Medzhitov, T. Horng, Transcriptional control of the inflammatory response. *Nat Rev Immunol* **9**, 692 (Oct, 2009).
 32. Y. H. Ho, P. Shah, Y. W. Chen, C. S. Chen, Systematic Analysis of Intracellular-targeting Antimicrobial Peptides, Bactenecin 7, Hybrid of Pleurocidin and Dermaseptin, Proline-Arginine-rich Peptide, and Lactoferricin B, by Using Escherichia coli Proteome Microarrays. *Mol Cell Proteomics* **15**, 1837 (Jun, 2016).
 33. Y. Lan *et al.*, Structural contributions to the intracellular targeting strategies of antimicrobial peptides. *Biochim Biophys Acta* **1798**, 1934 (Oct, 2010).
 34. R. W. Scott, G. N. Tew, Mimics of Host Defense Proteins; Strategies for Translation to Therapeutic Applications. *Curr Top Med Chem* **17**, 576 (2017).
 35. K. E. Greber, M. Dawgul, Antimicrobial Peptides Under Clinical Trials. *Curr Top Med Chem* **17**, 620 (2017).
 36. J. M. Sierra, E. Fuste, F. Rabanal, T. Vinuesa, M. Vinas, An overview of antimicrobial peptides and the latest advances in their development. *Expert Opin Biol Ther* **17**, 663 (Jun, 2017).
 37. R. M. Epand, C. Walker, R. F. Epand, N. A. Magarvey, Molecular mechanisms of

- membrane targeting antibiotics. *Biochim Biophys Acta* **1858**, 980 (May, 2016).
38. M. L. Mangoni, Y. Shai, Short native antimicrobial peptides and engineered ultrashort lipopeptides: similarities and differences in cell specificities and modes of action. *Cell Mol Life Sci* **68**, 2267 (Jul, 2011).
39. T. H. Lee, K. N. Hall, M. I. Aguilar, Antimicrobial Peptide Structure and Mechanism of Action: A Focus on the Role of Membrane Structure. *Curr Top Med Chem* **16**, 25 (2016).
40. M. Scocchi, M. Mardirossian, G. Runti, M. Benincasa, Non-Membrane Permeabilizing Modes of Action of Antimicrobial Peptides on Bacteria. *Curr Top Med Chem* **16**, 76 (2016).
41. M. Scocchi, A. Tossi, R. Gennaro, Proline-rich antimicrobial peptides: converging to a non-lytic mechanism of action. *Cell Mol Life Sci* **68**, 2317 (Jul, 2011).
42. S. T. Yang, S. Y. Shin, K. S. Hahm, J. I. Kim, Design of perfectly symmetric Trp-rich peptides with potent and broad-spectrum antimicrobial activities. *Int J Antimicrob Agents* **27**, 325 (Apr, 2006).
43. L. Otvos, Jr., Antibacterial peptides and proteins with multiple cellular targets. *J Pept Sci* **11**, 697 (Nov, 2005).
44. D. I. Chan, E. J. Prenner, H. J. Vogel, Tryptophan- and arginine-rich antimicrobial peptides: structures and mechanisms of action. *Biochim Biophys Acta* **1758**, 1184 (Sep, 2006).
45. J. S. Molton, P. A. Tambyah, B. S. Ang, M. L. Ling, D. A. Fisher, The global spread of healthcare-associated multidrug-resistant bacteria: a perspective from Asia. *Clin Infect Dis* **56**, 1310 (May, 2013).
46. C. L. Ventola, The antibiotic resistance crisis: part 1: causes and threats. *P T* **40**, 277 (Apr, 2015).
47. P. M. Hawkey, Multidrug-resistant Gram-negative bacteria: a product of globalization. *J Hosp Infect* **89**, 241 (Apr, 2015).
48. S. Vasoo, J. N. Barreto, P. K. Tosh, Emerging issues in gram-negative bacterial resistance: an update for the practicing clinician. *Mayo Clin Proc* **90**, 395 (Mar, 2015).

49. N. Papo, Y. Shai, A molecular mechanism for lipopolysaccharide protection of Gram-negative bacteria from antimicrobial peptides. *J Biol Chem* **280**, 10378 (Mar 18, 2005).
50. S. T. Yang *et al.*, Contribution of a central proline in model amphipathic alpha-helical peptides to self-association, interaction with phospholipids, and antimicrobial mode of action. *Febs J* **273**, 4040 (Sep, 2006).
51. B. Loh, C. Grant, R. E. Hancock, Use of the fluorescent probe 1-N-phenylnaphthylamine to study the interactions of aminoglycoside antibiotics with the outer membrane of *Pseudomonas aeruginosa*. *Antimicrob Agents Chemother* **26**, 546 (Oct, 1984).
52. R. I. Lehrer *et al.*, Interaction of human defensins with *Escherichia coli*. Mechanism of bactericidal activity. *J Clin Invest* **84**, 553 (Aug, 1989).
53. S. T. Yang, S. Y. Shin, K. S. Hahm, J. I. Kim, Different modes in antibiotic action of tritrypticin analogs, cathelicidin-derived Trp-rich and Pro/Arg-rich peptides. *Biochim Biophys Acta* **1758**, 1580 (Oct, 2006).
54. S. Kobayashi, K. Takeshima, C. B. Park, S. C. Kim, K. Matsuzaki, Interactions of the novel antimicrobial peptide buforin 2 with lipid bilayers: proline as a translocation promoting factor. *Biochemistry-US* **39**, 8648 (Jul 25, 2000).

PART II

Dimerization of host defense peptides: Benefits and drawbacks for therapeutic applications

1. Introduction

Host defense peptides (HDPs) are found in both unicellular and multicellular organisms and are the primary line of defense against invading pathogens (1-3). Due to their low resistance, HDPs are a promising alternative to conventional antibiotics in combating antibiotic-resistant bacterial infections (4-8). HDPs derived from multicellular organisms are capable of killing or inhibiting a wide variety of microorganisms, including gram-positive and gram-negative bacteria. The predominant mechanism of bacterial cell death induced by HDPs is via the permeabilization of the negatively charged cytoplasmic membrane (9-12). However, some HDPs have been suggested to exert their antimicrobial effects intracellularly by altering enzyme activity or binding to DNA (13, 14). For instance, while magainin II is a well-known membrane-permeabilizing AMP, buforin II exhibits potent antimicrobial activity without causing membrane lysis (15, 16). Confocal fluorescence microscopic studies have shown that magainin II localizes to the bacterial surface, whereas buforin II accumulates mainly in the cytoplasm (17).

The ability of membrane-active peptides to self-associate appears to be a critical factor in determining their antimicrobial mode of action, whether it involves membrane permeabilization or peptide translocation across the membrane to target intracellular components (18, 19). Numerous studies have demonstrated that dimerization of membrane-permeabilizing peptides significantly alters their biological and biophysical properties (20, 21). For instance, the parallel and antiparallel magainin II dimers exhibit greater biological activity and a stronger affinity for membranes than the monomeric form (22). Furthermore, the pore formed by the magainin II dimer has a larger diameter and

a longer lifespan than that of the monomer (23). Despite the potential benefits of dimerizing HDPs to enhance antimicrobial potency, dimerization of membrane-permeabilizing HDPs can increase cytotoxicity against mammalian cells (21), which should be minimized or eliminated. Conversely, although dimerization of cell-penetrating peptides enhances cellular uptake and drug delivery (24), little is currently known about their antimicrobial properties.

In this study, I synthesized magainin II, buforin II, and their corresponding homodimeric peptides with a branched Lys core, as listed in Table 1. I evaluated their antibacterial activities against gram-positive and gram-negative bacteria and their cytotoxicity against mammalian cells. I also examined the impact of dimerization on their antimicrobial properties and investigated their interactions with lipid bilayers in membrane mimetic environments using circular dichroism and fluorescence spectroscopy. My results demonstrated that the Lys-linked buforin II dimer exhibited superior antibacterial potency against both gram-positive and gram-negative bacteria, including several antibiotic-resistant bacterial isolates, without inducing any cytotoxicity against mammalian cells. I concluded that the dimerization of buforin II not only enhanced its membrane-permeabilizing and cell-penetrating abilities but also contributed to more efficient and selective eradication of pathogenic bacteria.

2. Materials and methods

2.1. *Materials and Microorganisms*

Novabiochem (Läufelfingen, Switzerland) provided N-fluoren-9-yl-methoxycarbonyl (Fmoc) amino acids that had orthogonal side chain protecting groups and Fmoc-Lys(Fmoc)-OH (for the dimeric peptides). Applied Biosystems (Foster City, CA, USA) provided the reagents and solvents required for peptide synthesis. The correct molecular weights of the peptides were confirmed by MALDI-TOF-MS (Shimadzu, Japan) after RP-HPLC purification that achieved above 99% purity. Avanti Polar Lipids (Alabaster, AL, USA) provided the phospholipids, while Molecular Probes, Inc. (Eugene, OR, USA) supplied a membrane potential-sensitive fluorescent dye, 3,3'-dipropylthiadicarbocyanine iodide [DiSC3(5)]. The microorganisms used in the study were purchased from the Korean Collection for Type Cultures (Daejeon, Korea).

2.2. *CD spectroscopy*

The J-715 spectrophotometer (Jasco, Japan) was used to collect the CD spectra of the peptides, following the previously described method (25). The spectra are expressed as the mean residue ellipticity $[\theta]$ versus wavelength. The ellipticity $[\theta]$ given in units of $\text{deg}\cdot\text{cm}^2\cdot\text{dmol}^{-1}$ was calculated using the following formula: $[\theta] = [\theta]_{\text{obs}} \text{MRW}/10lc$, where MRW = mean residue molecular weight of the peptide, c is the concentration of the sample, and l is the length of the cell.

2.3. *Antimicrobial, hemolytic and cytotoxic activity*

The broth microdilution method was used to measure the antimicrobial activity of peptides against gram-positive and gram-negative bacteria, including antibiotic-resistant strains, as described previously (14). In brief, a single colony of bacteria was cultured on an LB agar plate and then transferred to LB medium, where it was incubated overnight at 37°C. The resulting culture was diluted and added to 96-well microtiter plates, followed by a series of dilutions of peptides. After incubation at 37°C for 16 hours, the minimal inhibitory concentration (MIC) was determined by measuring the optical density (OD) at 600 nm. The hemolytic activities of peptides were determined by monitoring the release of hemoglobin from human red blood cells, as described previously (25). Complete hemolysis was induced by 0.1% Triton X-100. Cytotoxicity against RAW 264.7 cells was evaluated using a 3-(4,5-dimethylthiazol-2-yl)-2,5-diphenyltetrazolium bromide (MTT) assay, as previously reported (25). The cell viability was determined by calculating the ratio of the absorbance at 570 nm for peptide-treated cells to that of untreated cells.

2.4. Membrane depolarization induced by peptides

The peptides' membrane depolarization activities were evaluated using the membrane potential-sensitive fluorescent dye DiSC3(5), as previously outlined (26). *S. aureus* cells at mid-log phase were suspended in 5 mM HEPES buffer, and DiSC3(5) was added to the cell suspension, causing the fluorescence to quench and stabilize. Introduction of peptides (2 mM) raised the fluorescence intensity due to membrane depolarization. The fluorescence change of DiSC3(5) was measured at an excitation/emission wavelength of 620/670 nm using a Shimadzu RF-5301 spectrofluorometer, and the maximum fluorescence intensity

was observed after adding gramicidin D, which results in complete dissipation of the membrane potential after 5 minutes.

2.5. Membrane disruption induced by peptides

The extrusion method was used to generate large unilamellar vesicles (LUVs), and the impact of peptides on membrane disruption was assessed using the fluorescent dye calcein, following the previously described protocol (14). Specifically, peptides were introduced to LUVs containing calcein and composed of either anionic PC/PG (1:1) or zwitterionic PC. The membrane-lytic activity of peptides was calculated as the percentage of leakage from 100 M LUVs after 10 minutes of incubation with peptides (2 μ M for PC/PG (1:1) and 20 μ M for PC vesicles). Fluorescence changes resulting from calcein release from LUVs were measured on a Shimadzu RF-5301 spectrofluorometer at an excitation/emission wavelength of 490/520 nm. The maximum fluorescence intensity due to complete membrane permeability was established by adding Triton X-100.

2.6. Ability of peptides to translocate into vesicles

Large unilamellar vesicles (LUVs) were prepared in HEPES buffer (150 mM NaCl, pH 7.4) containing chymotrypsin (200 mM), according to previous methods (14). The addition of trypsin-chymotrypsin inhibitor (200 mM) was used to inactivate external chymotrypsin. The translocation of peptides into the vesicles was monitored by fluorescence transfer from the Trp residue of peptides to the dansyl group on membranes, and measured on a Shimadzu RF-5301 spectrofluorometer with excitation/emission wavelength set at 280/510 nm.

3. Results

3.1. *Circular dichroism (CD) studies*

To examine structural variations between monomeric and dimeric peptides in both aqueous and membrane-mimetic environments, CD spectroscopy was employed, as illustrated in Figure 1. In aqueous buffer, all peptides exhibited mostly disordered coil structures. Conversely, in SDS micelles, a membrane-mimetic environment, both monomeric and dimeric magainin II adopted standard α -helical structures, as evidenced by the double minima observed at 208 and 222 nm. In comparison to magainin II, which disrupts membranes, buforin II, which penetrates cells, had a negative peak at 204 nm, suggesting a somewhat different structure from a typical α -helix. However, the CD spectra of the monomers and dimers were comparable, indicating that dimerization did not significantly affect the peptides' structure.

3.2. *Antimicrobial and hemolytic activities of the peptides*

I proceeded to determine the peptides' ability to impede bacterial growth by measuring their MIC, which are summarized in Table 2. In comparison to their individual monomers, the magainin II dimer and the buforin II dimer exhibited an amplified antibacterial effect of 4-8 and 8-16 times, respectively. Furthermore, Table 3 illustrates that the dimers had potent antimicrobial activity, ranging from 0.5-4 μ M, against antibiotic-resistant pathogens. These findings suggest that the dimerization of not only membrane-permeabilizing magainin II but also cell-penetrating buforin II is an effective approach to enhance antimicrobial activity.

3.3. *Membrane depolarization by peptides*

In order to investigate the relationship between membrane depolarization and bacterial death, I conducted experiments to determine whether monomeric and dimeric peptides could depolarize the cytoplasmic membrane of *S. aureus* using the fluorescent dye DiSC3(5) as an indicator of membrane potential. As depicted in Fig. 2A, monomeric magainin II was effective at depolarizing the cytoplasmic membrane of *S. aureus* at concentrations lower than the MIC, whereas buforin II did not induce membrane depolarization even at the MIC concentration. Although there was no direct correlation between cytoplasmic membrane depolarization and MIC values, these findings suggest that magainin II's antimicrobial activity is associated with membrane depolarization, whereas the potent antimicrobial activity of buforin II is not related to membrane depolarization. Both monomeric and dimeric magainin II dissipated the membrane potential of *S. aureus*, with the magainin II dimer inducing more effective membrane depolarization than the monomer. Notably, the buforin II monomer displayed negligible membrane depolarization ability, while the buforin II dimer dissipated over 50% of membrane potential. These results indicate that the additional ability of buforin II dimer to induce membrane depolarization appears to be associated with its potent antimicrobial activity.

3.4. *Dye leakage from liposomes*

I conducted an experiment to investigate the ability of peptides to permeabilize membranes, focusing on their effect on anionic vesicles composed of L- α -phosphatidylcholine (PC) and L- α -phosphatidylglycerol (PG) (1:1) as well as zwitterionic vesicles composed of PC. I monitored the efflux of fluorescent dye

from the vesicles to assess membrane-lytic activity (Fig. 2B). My results were consistent with the peptides' respective abilities to depolarize bacterial membranes: magainin II showed strong calcein release from the PC/PG (1:1) vesicles, with 50% leakage at 2 M, while buforin II showed no membrane-lytic activity. These findings support the notion that membrane disruption is a key killing mechanism for magainin II but not for buforin II. Interestingly, neither peptide elicited any calcein release from PC liposomes, even at high concentrations, which is consistent with my findings for hemolytic and cytotoxic activity. Dimerization of magainin II significantly enhanced its membrane-lytic activity against both anionic and zwitterionic liposomes, indicating non-selective increases in membrane-lytic ability between negatively charged and neutral membranes. Conversely, the buforin II dimer had relatively strong membrane-lytic activity (~60%) against anionic liposomes but did not cause any dye leakage from PC liposomes, demonstrating selective membrane-disrupting activity only for anionic membranes. While the membrane-lytic activity of the peptides was related to their respective antimicrobial activity, I found that this relationship was not entirely linear.

3.5. *Ability of peptides to translocate into liposomes*

To assess the cellular uptake ability of peptides, I investigated their capacity to translocate through lipid bilayers (Fig. 3). I estimated the degree of peptide translocation across PC/PG/dansyl-PE (50:45:5) vesicles by measuring peptide degradation through chymotrypsin encapsulated within the vesicles using a fluorescence resonance energy transfer system with a Trp donor and dansyl acceptor. Magainin II showed no decrease in fluorescence throughout the 500 s,

indicating a lack of membrane translocation. On the other hand, buforin II caused a time-dependent decrease in fluorescence intensity, indicating effective penetration of the lipid bilayer and entry into the vesicles. These results are consistent with previously reported translocation findings. As with the monomers, the buforin II dimer translocated more efficiently and rapidly across the membrane than the magainin II dimer. These outcomes indicate that both monomeric and dimeric buforin II have the ability to cross the bacterial membrane and target intracellular molecules.

4. Discussion

The therapeutic potential of membrane-active molecules, such as antimicrobial and cell-penetrating peptides, has generated significant interest, leading to extensive research aimed at elucidating the fundamental principles of peptide interaction with cell membranes (27, 28). These molecules generally possess cationic and amphipathic properties that play vital roles in membrane permeabilization and cell penetration. The effects of peptide self-assembly on membrane permeabilization and cell penetration have been studied by various groups, highlighting the structural and biological differences between monomeric and dimeric forms (20, 24). Interestingly, dimerization of host defense peptides has been shown to enhance their antibiotic activity against several bacterial species (29-33). This improved activity is linked to an increase in membrane permeabilization, indicating that bacterial membranes are the primary targets of dimers. However, the cytotoxicity of dimers against mammalian cells can be increased when the peptides have membrane-permeabilizing modes of action, which limits their therapeutic potential (20, 21). My findings confirm that the membrane-permeabilizing magainin II dimer exhibits potent antibacterial activity but is also highly cytotoxic to mammalian cells. The improved activity of the magainin II dimer is associated with its strong membrane-lytic ability against anionic and zwitterionic membranes, respectively. Conversely, the membrane-penetrating buforin II dimer displays potent broad-spectrum antimicrobial activity without being cytotoxic to mammalian cells. Consistent with previous reports (17), the buforin II monomer inhibits bacterial cell growth without disrupting the membrane. However, the buforin II dimer has the ability to depolarize bacterial membranes, permeabilize anionic membranes, and translocate across lipid

membranes. These results, obtained using biological and artificial membranes, suggest that the buforin II dimer directly collapses the cytoplasmic membrane potential and also interferes with intracellular targets, which may contribute to its potent antibacterial activity.

To sum up, I investigated the effects of dimerization on magainin II, a membrane-permeabilizing peptide, and buforin II, a membrane-penetrating peptide. The magainin II dimer showed increased antibacterial and cytotoxic effects, while the buforin II dimer enhanced antibacterial activity without causing any harm to mammalian cells. Furthermore, the buforin II dimer demonstrated the ability to depolarize bacterial membranes and translocate across lipid bilayers to target intracellular components, making it a promising candidate for therapeutic control of multi-resistant pathogenic bacteria due to its wide range of antimicrobial activity against gram-positive and gram-negative bacteria, including antibiotic-resistant isolates. Although further research is required to determine the exact mechanism of action of the buforin II dimer, dimerization of HDPs that target intracellular components may be a promising strategy for improving antimicrobial activity while reducing cytotoxicity against mammalian cells.

Table 1. Amino acid sequences and cytotoxic activities of peptides used in this study

Peptides	Amino acid sequences	HC ₅₀ ^a	LC ₅₀ ^b
magainin II	GIGKWLHSAKKFGKAFVGEIMNS	> 200	> 200
K-(magainin II) ₂	(GIGKWLHSAKKFGKAFVGEIMNS) ₂ K	14.3	2.7
buforin II	TRSSRAGLQWPVGRVHRLLRK	> 200	> 200
K-(buforin II) ₂	(TRSSRAGLQWPVGRVHRLLRK) ₂ K	> 200	> 200

^aPeptide concentration (μM) causing 50% hemolysis.

^bPeptide concentration (μM) causing 50% growth inhibition of RAW 264.7 cells.

Table 2. Antimicrobial activities of peptides against Gram-positive and Gram-negative bacteria

Organism	Antimicrobial activity (MIC: μM)			
	magainin II	K-(magainin II) ₂	buforin II	K-(buforin II) ₂
Gram-positive bacteria				
<i>Bacillus subtilis</i>	8	2	8	0.5
<i>Staphylococcus aureus</i>	16	2	8	1
<i>Staphylococcus epidermidis</i>	16	4	16	2
Gram-negative bacteria				
<i>Escherichia coli</i>	32	4	8	1
<i>Salmonella Typhimurium</i>	16	2	4	0.5
<i>Pseudomonas aeruginosa</i>	32	4	16	2

Table 3. Antimicrobial activities of peptides against antibiotic-resistant bacterial isolates.

Antibiotic-resistant bacteria	Antimicrobial activity (MIC: μM)			
	magainin II	K-(magainin II) ₂	buforin II	K-(buforin II) ₂
Methicillin-resistant <i>Staphylococcus aureus</i> (1) [MRSA (1)]	16.0	4.0	8.0	1.0
Methicillin-resistant <i>Staphylococcus aureus</i> (2) [MRSA (2)]	16.0	2.0	8.0	0.5
Vancomycin-resistant <i>Enterococcus faecalis</i> (1)	32.0	4.0	16.0	1.0
Vancomycin-resistant <i>Enterococcus faecalis</i> (2)	16.0	4.0	8.0	1.0

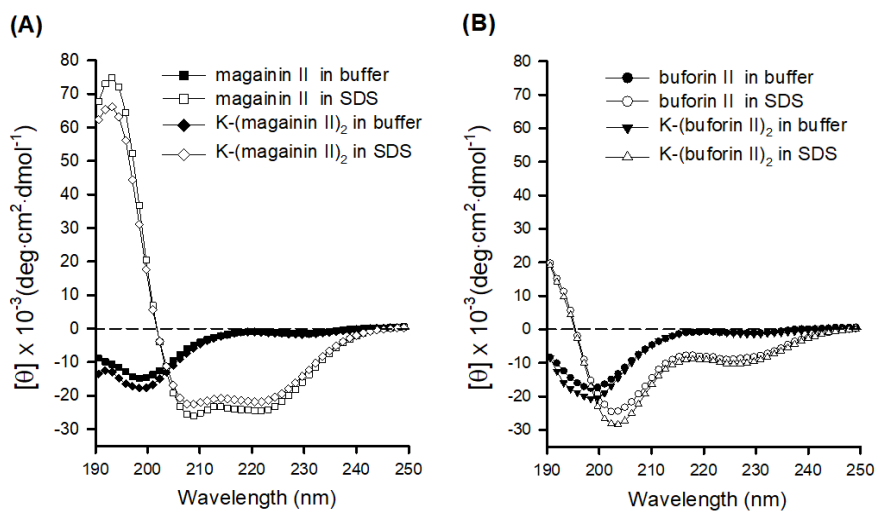


Fig. 1. CD spectra of the peptides. The CD spectra of magainin II and K-(magainin II)₂ (A) and buforin II and K-(buforin II)₂ (B) were obtained at 25 °C in 10 mM sodium phosphate buffer (open symbols), or 30 mM SDS micelles (closed symbols). Spectra were taken at peptide concentrations of 20 μM.

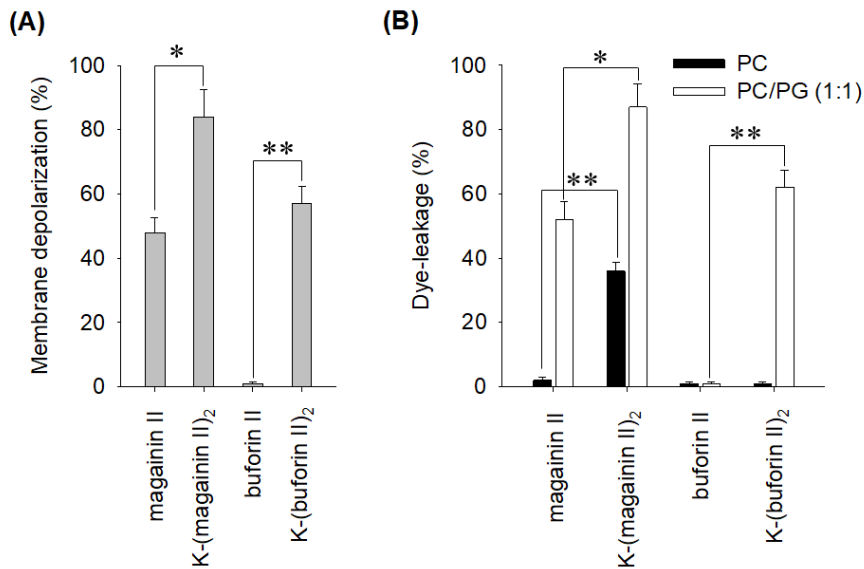


Fig. 2. Ability of peptides to permeabilize membranes. (A) Effect of peptides on membrane potential of intact *S. aureus* cells (OD600 = 0.05). After the fluorescence of DiSC3(5) was stabilized, the peptides (2 μ M) were added to *S. aureus*. (B) Release of calcein fluorescent probe from anionic PC/PG (1:1) or zwitterionic PC vesicles. Membrane-lytic activity of peptides was defined as the percent leakage from 100 μ M lipid after 10 min incubation with peptides (2 μ M for PC/PG (1:1) and 20 μ M for PC vesicles). Average \pm SD for three independent experiments. Statistically significant ($p < 0.05$) and very significant ($p < 0.01$) differences are represented by (*) and (**), respectively

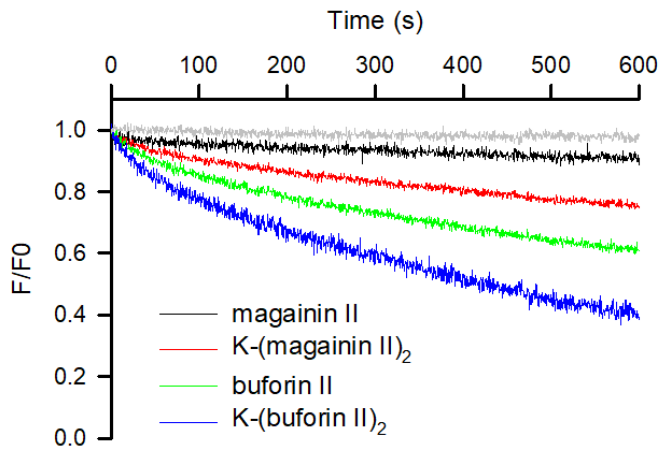


Fig. 3. Ability of peptides to translocate into liposomes. Membrane translocation of peptides was measured by resonance energy transfer from Trp to DNS-PE. Decreased fluorescence means that the peptide has entered the vesicle. Lipid and peptide concentrations were 100 and 1 μ M, respectively.

References

1. E. F. Haney, S. K. Straus, R. E. W. Hancock, Reassessing the host defense Peptide Landscape. *Front Chem* **7**, 43 (2019).
2. A. L. Hilchie, K. Wuerth, R. E. Hancock, Immune modulation by multifaceted cationic host defense (antimicrobial) peptides. *Nat Chem Biol* **9**, 761 (Dec, 2013).
3. L. J. Zhang, R. L. Gallo, Antimicrobial peptides. *Curr Biol* **26**, R14 (Jan 11, 2016).
4. M. Mahlapuu, J. Hakansson, L. Ringstad, C. Bjorn, Antimicrobial peptides: An Emerging Category of Therapeutic Agents. *Front Cell Infect Microbiol* **6**, 194 (2016).
5. K. Lohner, Membrane-active Antimicrobial peptides as Template Structures for Novel Antibiotic Agents. *Curr Top Med Chem*, (Jul 13, 2016).
6. L. S. Biswaro, M. G. da Costa Sousa, T. M. B. Rezende, S. C. Dias, O. L. Franco, Antimicrobial peptides and Nanotechnology, Recent Advances and Challenges. *Front Microbiol* **9**, 855 (2018).
7. A. de Breij *et al.*, The host defense peptide SAAP-148 combats drug-resistant bacteria and biofilms. *Sci Transl Med* **10**, (Jan 10, 2018).
8. P. Kumar, J. N. Kizhakkedathu, S. K. Straus, Antimicrobial peptides: Diversity, Mechanism of Action and Strategies to Improve the Activity and Biocompatibility In Vivo. *Biomolecules* **8**, (Jan 19, 2018).
9. T. A. Stone *et al.*, Positive Charge Patterning and Hydrophobicity of Membrane-Active host defense peptides as Determinants of Activity, Toxicity, and Pharmacokinetic Stability. *J Med Chem*, (Jul 1, 2019).
10. S. Guha, J. Ghimire, E. Wu, W. C. Wimley, Mechanistic Landscape of Membrane-Permeabilizing Peptides. *Chem Rev*, (Jan 9, 2019).
11. M. A. Sani, F. Separovic, How Membrane-Active Peptides Get into Lipid Membranes. *Acc Chem Res* **49**, 1130 (Jun 21, 2016).
12. K. Matsuzaki, Membrane Permeabilization Mechanisms. *Adv Exp Med Biol* **1117**, 9 (2019).
13. C. F. Le, C. M. Fang, S. D. Sekaran, Intracellular Targeting Mechanisms by Antimicrobial peptides. *Antimicrob Agents Chemother* **61**, (Apr, 2017).
14. H. Lee *et al.*, Conjugation of Cell-Penetrating Peptides to Antimicrobial peptides Enhances Antibacterial Activity. *ACS Omega* **4**, 15694 (Sep 24, 2019).

- 15.K. Takeshima, A. Chikushi, K. K. Lee, S. Yonehara, K. Matsuzaki, Translocation of analogues of the antimicrobial peptides magainin and buforin across human cell membranes. *J Biol Chem* **278**, 1310 (Jan 10, 2003).
- 16.Y. Imura, N. Choda, K. Matsuzaki, Magainin 2 in action: distinct modes of membrane permeabilization in living bacterial and mammalian cells. *Biophys J* **95**, 5757 (Dec 15, 2008).
- 17.C. B. Park, K. S. Yi, K. Matsuzaki, M. S. Kim, S. C. Kim, Structure-activity analysis of buforin II, a histone H2A-derived antimicrobial peptide: the proline hinge is responsible for the cell-penetrating ability of buforin II. *Proc Natl Acad Sci U S A* **97**, 8245 (Jul 18, 2000).
- 18.S. T. Yang *et al.*, Contribution of a central proline in model amphipathic alpha-helical peptides to self-association, interaction with phospholipids, and antimicrobial mode of action. *Febs J* **273**, 4040 (Sep, 2006).
- 19.P. Petkov, E. Lilkova, N. Ilieva, L. Litov, Self-Association of antimicrobial peptides: A Molecular Dynamics Simulation Study on Bombinin. *Int J Mol Sci* **20**, (Nov 1, 2019).
- 20.E. N. Lorenzon, J. P. Piccoli, N. A. Santos-Filho, E. M. Cilli, Dimerization of Antimicrobial peptides: A Promising Strategy to Enhance host defense peptide Activity. *Protein Pept Lett* **26**, 98 (2019).
- 21.S. Gunasekera, T. Muhammad, A. A. Stromstedt, K. J. Rosengren, U. Goransson, Backbone Cyclization and Dimerization of LL-37-Derived Peptides Enhance Antimicrobial Activity and Proteolytic Stability. *Front Microbiol* **11**, 168 (2020).
- 22.Y. Mukai, Y. Matsushita, T. Niidome, T. Hatekeyama, H. Aoyag, Parallel and antiparallel dimers of magainin 2: their interaction with phospholipid membrane and antibacterial activity. *J Pept Sci* **8**, 570 (Oct, 2002).
- 23.T. Hara *et al.*, Effects of peptide dimerization on pore formation: Antiparallel disulfide-dimerized magainin 2 analogue. *Biopolymers* **58**, 437 (Apr 5, 2001).
- 24.J. Hoyer, U. Schatzschneider, M. Schulz-Siegmund, I. Neundorf, Dimerization of a cell-penetrating peptide leads to enhanced cellular uptake and drug delivery. *Beilstein J Org Chem* **8**, 1788 (2012).
- 25.S. Yang *et al.*, Structural analysis and mode of action of BMAP-27, a cathelicidin-derived host defense peptide. *Peptides* **118**, 170106 (Aug, 2019).

- 26.S. T. Yang, S. Y. Shin, K. S. Hahm, J. I. Kim, Different modes in antibiotic action of tritrypticin analogs, cathelicidin-derived Trp-rich and Pro/Arg-rich peptides. *Biochim Biophys Acta* **1758**, 1580 (Oct, 2006).
- 27.F. G. Avci, B. S. Akbulut, E. Ozkirimli, Membrane Active Peptides and Their Biophysical Characterization. *Biomolecules* **8**, (Aug 22, 2018).
- 28.S. T. Henriques, M. N. Melo, M. A. Castanho, Cell-penetrating peptides and antimicrobial peptides: how different are they? *Biochem J* **399**, 1 (Oct 1, 2006).
- 29.A. Thamri *et al.*, Peptide modification results in the formation of a dimer with a 60-fold enhanced antimicrobial activity. *PLoS One* **12**, e0173783 (2017).
- 30.B. Liu *et al.*, Design of novel host defense peptide dimer analogues with enhanced antimicrobial activity in vitro and in vivo by intermolecular triazole bridge strategy. *Peptides* **88**, 115 (Feb, 2017).
- 31.J. J. Koh *et al.*, Design and synthesis of oligo-lipidated arginyl peptide (OLAP) dimers with enhanced physicochemical activity, peptide stability and their antimicrobial actions against MRSA infections. *Amino Acids* **50**, 1329 (Oct, 2018).
- 32.P. V. Panteleev, M. Y. Myshkin, Z. O. Shenkarev, T. V. Ovchinnikova, Dimerization of the antimicrobial peptide arenicin plays a key role in the cytotoxicity but not in the antibacterial activity. *Biochem Biophys Res Commun* **482**, 1320 (Jan 22, 2017).
- 33.E. N. Lorenzon *et al.*, The "pre-assembled state" of magainin 2 lysine-linked dimer determines its enhanced antimicrobial activity. *Colloids Surf B Biointerfaces* **167**, 432 (Jul 1, 2018).

PART III

Importance of structural arrangements of hydrophobic, amphipathic, and cationic domains in host defense peptides for antimicrobial activity

1. Introduction

The spread of antibiotic-resistant microorganisms causes human health problems worldwide, so extensive efforts have been made to develop new antimicrobial agents to overcome multidrug-resistant bacterial infections (1-3). Host defense peptides (HDPs) have broad-spectrum bacteriostatic and/or bactericidal effects against gram-positive and gram-negative species. Importantly, because of the low risk of developing antimicrobial resistance, HDPs are considered as a promising alternative antibiotic group to overcome the emergence of widespread antibiotic resistance (4-10). It is commonly thought that the primary mode of action for HDPs is their interaction with the cytoplasmic membrane of target pathogens, which causes membrane permeabilization and ultimately leads to cell death (11-14). Many studies on peptide-lipid interactions using several lipid model systems have been performed to elucidate key aspects of the mode of action of HDPs (15, 16). The lytic process of HDPs, which share common structural features of being cationic and amphipathic, is widely recognized to occur in two stages (17). In the first stage, the positively charged residues of the peptides interact with the negatively charged phospholipid headgroups, which is critical for the binding process of the peptide to the membrane. Then, the hydrophobic region of HDPs inserts into the hydrophobic core of the lipid bilayers, resulting in the lysis of the pathogenic membrane. However, the nonspecific interactions of HDPs with membranes can also result in cytotoxicity towards mammalian cells, limiting their clinical potential.

The antimicrobial selectivity of HDPs with an amphipathic α -helical structure is influenced by their structural flexibility and local backbone distortion (18, 19). HDPs with a helix-hinge-helix structure have been found to exhibit strong antibacterial activity without causing cytotoxicity, making the helix-hinge-helix structure a key feature for achieving antibacterial selectivity (20). In the previous

research, I demonstrated that helix-hinge-helix peptides possess selective and potent antimicrobial activity, with the hinge located near the middle of amphipathic α -helical peptides facilitating efficient peptide-membrane interactions (21).

The PXXP motif is a conserved sequence found in many HDPs. It consists of a proline (P) followed by any two amino acids (X), and another proline (P). The proline residues in the PXXP motif impart a unique structural feature to HDPs, as proline is known to disrupt the regular α -helical structure. A central hinge induced by PXXP motif is an important structural element in many HDPs, and its presence can significantly affect the activity and structure of the peptides (21, 22). The central PXXP motif leads to increased flexibility and mobility of the peptide chain, allowing the HDPs to more effectively interact with the lipid bilayer of microbial cell membranes. Understanding the role of the PXXP motif in these peptides can provide insights into their mechanism of action and help to guide the development of new antimicrobial agents based on HDPs.

In this study, I prepared three model amphipathic α -helical peptides containing a central hinge motif and investigated their structural, biological, and physicochemical properties. I prepared a continuous amphipathic α -helical peptide (KL) and three helix-hinge-helix peptides (KL-KL, KL-L, and KL-K) containing a central hinge PXXP motif, and investigated the biological, structural, and physicochemical properties. I will discuss in detail the importance of structural arrangements of hydrophobic, amphipathic, and cationic domains in HDPs for antimicrobial activity.

2. Materials and methods

2.1 *Materials and microorganisms*

The peptides were prepared by solid-phase peptide synthesis methods using fluorenylmethoxycarbonyl (Fmoc) chemistry and validated with reversed-phase high-performance liquid chromatography, as described previously (16, 23). N- α -Fmoc amino acids were purchased from Novabiochem (Laufelfingen, Switzerland) and other reagents for peptide synthesis were purchased from Applied Biosystems (Foster City, CA, USA). Fluorescent probes and phospholipids including phosphatidylglycerol (PG), phosphatidylserine (PS) and phosphatidylcholine (PC) were purchased from Invitrogen (Carlsbad, CA, USA) and Avanti Polar Lipids (Alabaster, AL, USA), respectively. Gram-positive (*S. aureus* and *B. subtilis*) and gram-negative (*E. coli* and *P. aeruginosa*) bacterial strains were obtained from the KCTC (Daejeon, South Korea).

2.2 *Circular dichroism (CD) spectroscopy*

The CD spectra of peptides were measured in a Jasco J-810 spectropolarimeter as described previously (22). Briefly, peptides dissolved in sodium phosphate buffer and in 30 mM sodium dodecyl sulphate (SDS) micelle were loaded into a 0.1 cm quartz cell and wavelengths were scanned from 190 to 250 nm with 50 nm/min speed, 0.1 nm step resolution, and 1 nm bandwidth. The spectra are presented as the mean residue ellipticity $[\theta]$, measured in units of $\text{deg}\cdot\text{cm}^2\cdot\text{dmol}^{-1}$ as a function of wavelength.

2.3 MIC determination

The antimicrobial activity of the peptides was determined against gram-positive *S. aureus* and *B. subtilis*, and gram-negative *E. coli*, and *P. aeruginosa* by the standard microdilution methods of the Clinical and Laboratory Standard Institute (CLSI) (24). Briefly, a colony of bacteria was incubated in Mueller Hinton (MH) broth in a 37°C shaking incubator for 24 h. An aliquot (50 µL) of the culture was transferred to fresh 10 mL MH broth, grown to reach the mid-logarithmic phase, and diluted with MHB to a bacterial count of 2×10^6 CFU ml⁻¹. A total of 100 µL of bacteria were added to 96-well microtiter plates in the presence of serial dilutions of peptides and incubated overnight at 37°C. The minimal inhibitory concentration (MIC) was expressed as the lowest concentration of peptides at which the bacteria did not grow by more than 90 %. Experiments were conducted in triplicate and repeated trice.

2.4 Time-killing kinetics assay

The time-kill experiments were performed according to CLSI guidelines, as described previously (25). Briefly, gram-positive *S. aureus* and gram-negative *E. coli* grown to the mid-logarithmic phase were diluted in LB broth to obtain a cell density of approximately 2×10^6 CFU/mL. The peptides were added to the bacterial cells and incubated at 37°C. Aliquots (100 µL) were drawn at different time intervals, plated after dilution on LB agar plates, and incubated at 37°C for 24 h to allow full colony development for calculating the viability of cells. The killing rate was plotted as the log CFU/mL over time. Experiments were repeated trice and their results were averaged.

2.5 Membrane depolarization

The measurement of membrane potential was conducted utilizing the voltage-sensitive fluorescent dye diSC3(5), as described previously (26, 27). Briefly, *S. aureus* was grown to the exponential phase at 37°C and resuspended at 1×10^8 CFU/mL in 20 mM HEPES buffer (100 mM KCl, pH 7.2). Fluorescence intensity was monitored at 670 nm (excited at 622 nm) on an RF-5301 spectrofluorometer (Shimadzu, Tokyo, Japan). The membrane potential of *S. aureus* was completely dissipated by adding gramicidin D. Experiments were repeated trice and their results were averaged.

2.6 Peptide-induced dye leakage form liposomes

Membrane disruption was investigated using the calcein leakage assay, as described previously (22). Briefly, the lipid film was hydrated in a solution containing 70 mM calcein in 20 mM HEPES buffer. After extruding the suspension through 100 nm polycarbonate filter, unencapsulated calcein was removed by passing liposomes through a Sephadex G-50 column. To evaluate the effect of peptides on membrane disruption, the release of calcein from the liposomes was measured by examining the fluorescence intensity at 520 nm (excited at 490 nm) using a Shimadzu RF-5301 spectrofluorometer. To determine the percentage of calcein release caused by the peptides, the following equation was used: Leakage (%) = $100 \times (F - F_0)/(F_t - F_0)$, where F_0 is the initial fluorescence intensity in the buffer, F and F_t are the fluorescence intensities after exposure to the peptide and 0.1% Triton X-100, respectively. Experiments were repeated trice and their results were averaged.

2.7 Tryptophan (Trp) fluorescence

Trp fluorescence measurements were used to estimate the binding of peptides to membranes, as described previously (28). Briefly, small unilamellar vesicles (SUVs) were generated by sonication and the peptides were added to the vesicles at a peptide/lipid molar ratio of 1:100. The mixture was then incubated for 10 minutes to allow for interaction. The Trp emission spectra of peptides were recorded at 300–400 nm. Experiments were repeated trice and their results were averaged

2.8 Cytotoxicity against erythrocytes

To determine the hemolytic activity of the peptides against sheep erythrocytes, the release of hemoglobin was measured after incubation with various peptide concentrations, as described previously (29). Briefly, fresh sheep erythrocytes were collected by centrifugation ($1,500 \times g$) for 10 min, washed twice with PBS (pH 7.2), and diluted to a concentration of 4% in the buffer. Erythrocytes were introduced to a 96-well plate in the presence of peptides and incubated at 37°C for 1 hour. The plates were then centrifuged at $1,000 \times g$ for 5 minutes, and the resulting supernatant was transferred to a new 96-well plate. The hemolytic activity of the peptides was evaluated by using an ELISA microplate reader to measure the absorbance of the supernatant at 414 nm, indicative of hemoglobin release. A zero hemolysis control was established using PBS, while 0.1% Triton X-100 resulted in complete (100%) hemolysis. Experiments were repeated trice and their results were averaged.

3. Results

3.1 Peptide design and structure

I generated four AHPs with different arrangements with amphipathic, hydrophobic and cationic domains; continuous amphipathic helix (KL), amphipathic–amphipathic domain (KL-KL), amphipathic–hydrophobic domain (KL-L), and amphipathic–cationic domain (KL-K). KL-KL, KL-L, and KL-K contain a PXXP motif connecting N- and C-terminal domains. A single Trp residue was introduced in position 2 of these peptides to allow fluorescent determination of their concentration and peptide-lipid interactions. The structural diagrams and characteristics of the peptides are shown in Fig. 1. CD spectroscopy was used to monitor the secondary structure of the peptides. The CD spectra of peptides were collected in 50 mM sodium phosphate buffer, or 30 mM SDS micelles (Figure 2). The CD spectra of all of the peptides indicated α -helix structures in the presence of SDS micelles (Figure 2C), but there was large difference in the helical contents between the peptides. As expected, compared to KL, PXXP-containing peptides have a partially distorted helix structure in membrane-mimetic environments. Interestingly, in aqueous buffer, KL and KL-L exhibited typical α -helical CD spectra, with minimal mean residue molar ellipticity values at 208 and 222 nm, whereas the CD spectra of KL-KL and KL-K had a negative band below 200 nm, indicating a lack of ordered structure.

3.2 Antimicrobial and hemolytic activity

Table 1 displays the antibacterial activity of the peptides designed derivatives as minimal inhibitory concentration (MIC) against gram-positive bacteria,

including *B. subtilis*, *S. aureus*, and *S. epidermidis* as well as gram-negative bacteria, including *E. coli*, *S. typhimurium*, and *P. aeruginosa*. KL exhibited activity with MIC values in the 16–32 μM range but was inactive against *S. epidermidis* and *P. aeruginosa*. Importantly, KL-KL were found to be more potent against both gram-positive and gram-negative bacteria than KL, with MIC values in the 2 to 4 μM range. Although both KL-L and KL-K exerted antimicrobial activity better than o KL, KL-K had the most potent antimicrobial activity among the peptides used in this study. To evaluate the cell-selectivity of the peptides, I measured hemolytic activity against sheep erythrocytes. Both KL and KL-L showed strong hemolytic activities although KL was more cytotoxic than KL-L. Interestingly, KL-KL and KL-K were not hemolytic. These results indicate that the arrangement with amphipathic, hydrophobic and cationic domains are critical for antimicrobial potency and selectivity.

To further investigate the differences in their lethal effects, I measured the time-dependent behavior of their bactericidal activity against *S. aureus* and *E. coli*, which are examples of gram-positive and gram-negative bacteria, respectively. The number (CFUs/ml) of viable bacterial cells trended to decrease with time, after treatment with peptides to the bacteria (Fig. 2). At the 2 x MIC, KL-KL and KL-K had little immediate impact on the number of surviving CFUs which were reduced by less than only 25% after 120 min of incubation. By contrast, it was observed that KL-L almost completely killed both bacteria within 60 min. Killing kinetics studies of the peptides on *S. aureus* and *E. coli* demonstrated that the hydrophobic C-terminal α -domain has a drastic effect on the rapid killing of the peptides.

3.3 Membrane depolarization and permeabilization

The bactericidal activity of HDPs is often associated with membrane depolarization and permeabilization. To investigate whether antimicrobial activity by the peptides is related to membrane depolarization, the ability to depolarize the cell membrane of *S. aureus* was evaluated (Fig. 3a). Interestingly, I found that KL and KL-L were much higher than KL-KL and KL-K, indicating that the hydrophobic C-terminal helix has a significant effect on their membrane depolarizing activity. The correlation between bactericidal activity and membrane depolarization of the peptides suggests that loss of membrane potential may be a major contributor to the bactericidal effect. I then generated calcein-containing liposomes composed of PG/PC (1:1) and investigated the ability of the peptides to induce membrane permeabilization by measuring the release of entrapped calcein from the liposomes into an aqueous buffer (Fig. 3b). Similar to their ability to depolarize bacterial membranes, KL-KL and KL-K induced weak calcein release (~30%) from liposomes, whereas KL and KL-L showed strong membrane-lytic activity (70~80%), which further confirmed that the C-terminal domain plays important roles in efficient membrane permeabilization. KL-L with the most potent bactericidal activity showed the greatest membrane depolarization and permeabilization, suggesting that membrane disruption is the primary event in bacterial killing for KL-L. In addition my results suggests that the central hinge region, which is an important structural component, enables a separation between the N-terminal interaction and the C-terminal interaction with the target cell membranes.

3.4 Binding of peptides to membranes by Trp fluorescence analysis

Because the intensity and emission maximum of Trp fluorescence are highly responsive to changes in the environment surrounding Trp residues, I utilized Trp fluorescence properties to estimate the partition of peptides into lipid membranes. Fig. 5 shows the Trp fluorescence emission spectra and maximum wavelength (λ_{\max}) for the peptides in buffer and in the presence of vesicles composed of PC/PG (1:1), or PC, at a peptide/lipid molar ratio of 1:100. The λ_{\max} value of KL-KL and KL-K in aqueous buffer was about 352 nm, indicating that Trp residues were exposed to a hydrophilic environment. In contrast, the λ_{\max} range of KL and KL-L was 343-345 nm, indicating that the peptides are self-assembled in buffer. In the presence of PC/PG (1:1) vesicles, all peptides caused a significant blue shift in the emission maximum, indicating that they bind to the negatively charged membranes. In contrast, although both KL and KL-L resulted in an intermediate blue shift, the addition of KL-KL and KL-K to PC liposomes only caused a minor shift (0-2 nm) in the Trp emission maxima. These findings explain why the peptides have a selective antimicrobial effect due to the fact that eukaryotic membranes are mostly made up of zwitterionic phospholipids, while prokaryotic membranes are composed of a combination of negatively charged and zwitterionic phospholipids.

4. Discussion

Amphipathic α -helical peptides (AHPs) are a promising class of antimicrobial agents with broad-spectrum activity against various bacterial pathogens. They disrupt bacterial cell membranes, making them less likely to induce bacterial resistance compared to traditional antibiotics that target specific cellular components (30-32). However, AHPs' nonspecific interactions with membranes can result in cytotoxicity towards mammalian cells, limiting their clinical potential. Developing selective AHPs with potent antimicrobial activity and reduced cytotoxicity is a significant challenge in antimicrobial drug discovery. Researchers have used model AHPs and artificial membranes to analyze the molecular structure-function relationships, understand peptide-lipid interactions, and identify the parameters that control cell selectivity (33). The length of the peptide chain, the tendency to form helices, the degree of amphipathicity, the overall positive charge, the level of hydrophobicity, and the hydrophobic moment are some factors that can affect their antibiotic activity. Although AHPs primarily disrupt membranes, some AHPs have an intracellular mechanism of action by binding to DNA or altering enzyme activities (34). This suggests that AHPs have a secondary mechanism of action to eliminate invading pathogens. Membrane permeabilization and cell penetration play key roles in the effective antimicrobial activity of AHPs, but the factors that regulate these two functions are not yet well understood.

The flexible region that connects the N- and C-terminal domains in AHPs is known as the central hinge, and it plays a crucial role in the peptide's mechanism of action. This region contains one or more proline residues, which impart flexibility to the peptide backbone, allowing it to undergo conformational

changes. These changes are essential for the peptide to interact with and disrupt the microbial membrane. The central hinge's flexibility allows the peptide to adopt various conformations, enabling it to insert into the membrane, disturb its integrity and penetrate across the membrane. Additionally, the orientation of the peptide on the membrane surface may be influenced by the central hinge, which can further enhance its antimicrobial activity. I showed that the central PXXP motif is crucial for providing structural flexibility and amphipathicity to PMAP-23, which plays a key role in its antimicrobial potency and selectivity by enabling it to interact preferentially with negatively charged membranes (16, 23).

In this study, I conducted research on AHPs that contain a central PXXP motif and explored their structural, biological, and physicochemical characteristics. My findings suggest that the central PXXP motif plays a crucial role in selective antimicrobial activity. Specifically, I found that KL-KL had significantly higher antimicrobial activity compared to KL, and that KL-L killed both *S. aureus* and *E. coli* rapidly. Among the PXXP-containing AHPs, my results indicate that KL-L was more effective at dissipating membrane potential in *S. aureus* and inducing leakage of calcein from LUVs than KL-KL. This may be due to the insertion of the hydrophobic C-terminal domain into the membrane, which caused efficient membrane depolarization and permeabilization. On the other hand, KL-K showed lower membrane permeabilization, but it was still highly active against both gram-positive *S. aureus* and gram-negative *E. coli* in bacterial growth inhibition tests. This suggests that KL-K may have a secondary target to inhibit bacterial growth after entering the cells, and the cationic C-terminal domain may play a role in the translocation of KL-K across the membrane. Interestingly, KL-K, which has structural similarities with HDP-CPP,

may share similar mechanisms of action. The recent findings indicate that CPP conjugation to HDPs facilitates translocation across the membrane and entry into bacterial cells and increase affinity to DNA due to the high positive charge of the conjugates. Like HDP-CPP conjugates, the increased antimicrobial activity observed for the KL-K could be explained by membrane disruption coupled to secondary intracellular targeting. The central hinge can affect the selectivity of AHPs between prokaryotic and eukaryotic cells. The arrangement of the N- and C-terminal domains can affect the interactions of the AHPs with microbial membranes. The arrangement of the N- and C-terminal domains connecting the central hinge can affect membrane permeabilization and translocation of AHPs. Although the antimicrobial efficacy of the peptides is related to a complex mode of action beyond simply membrane permeabilization, understanding the interactions of the helix-hinge-helix peptides with lipid bilayers is of great importance for antimicrobial drug development.

In conclusion, the helix-hinge-helix peptides demonstrated improved antibacterial activity and reduced hemolytic activity compared to the continuous helical KL. However, they exhibited significant differences in antibacterial activity and membrane permeabilization. KL-K was the most effective against both gram-positive and gram-negative bacteria, without any hemolytic activity. Although KL-L could kill bacteria after 30 minutes of exposure, it was less effective than KL-K. KL-L rapidly and strongly dissipated the membrane potential, while KL-K did not perturb the membrane significantly. These findings suggest that the arrangement of hydrophobic and cationic domains plays a crucial role in both membrane permeabilization and cell penetration, which are linked to bactericidal and bacteriostatic activity. A thorough understanding of the

interaction of peptides with various helix-hinge-helix structures with lipid bilayers could facilitate the design of highly selective and potent HDPs as effective antimicrobial drugs in the future. I propose that helix-hinge-helix peptides offer a promising approach for developing antibacterial agents with desirable properties.

Table 1 Amino acid sequence, molecular weight, net charge, and hydrophobicity of the peptides used in this study.

Peptides	Amino acid sequence	MW ^a	Net charge	Rt ^b
KL	KWLKLLKLLKLLKLLK	2262.0	+9	30.80
KL-KL	KWLKLLKPLKPLLKLLK	2214.9	+8	21.68
KL-L	KWLKLLKPLKPLLLLLL	2169.9	+5	28.84
KL-K	KWLKLLKPLKPKKKKKK	2260.0	+11	14.81

^aThe molecular weight of peptides was confirmed using ESI-LC-MS

^bRetention time (Rt) was measured using a C-18 reversed-phase analytical HPLC column.

Table 2. Antimicrobial activities of peptides against Gram-positive and Gram-negative bacteria.

Organism	Antimicrobial activity (MIC: μ M)			
	KL	KL-KL	KL-L	KL-K
Gram-positive bacteria				
<i>B. subtilis</i>	16	4	8	2
<i>S. aureus</i>	16	4	16	4
<i>S. epidermidis</i>	>64	4	8	2
Gram-negative bacteria				
<i>E. coli</i>	32	4	8	2
<i>S. typhimurium</i>	32	2	4	4
<i>P. aeruginosa</i>	>64	4	8	4

^a MIC (minimum inhibitory concentration) was determined as the lowest concentration of peptide that caused 100 % inhibition of microbial growth.

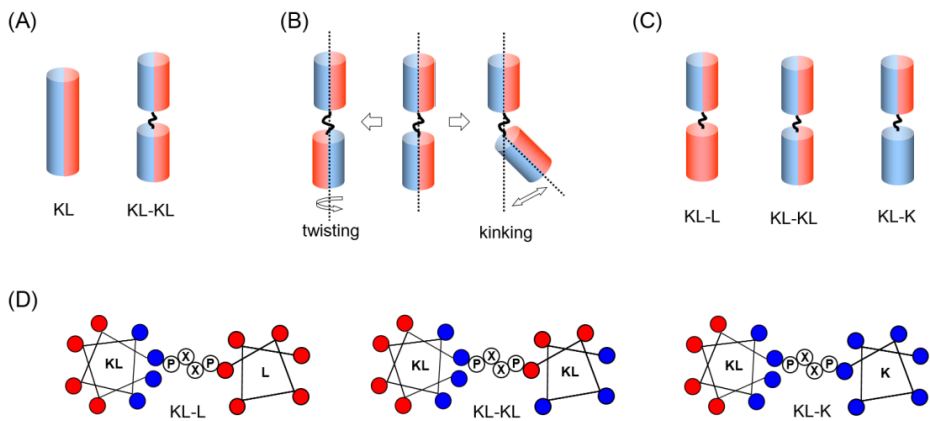


Fig. 1. Structural isomers of amphipathic α -helical peptides. (A) Schematic representation of continuous α -helix and helix-hinge-helix with amphipathic characteristics. Each helix is amphipathic, with a hydrophobic and a hydrophilic face. (B) Two possible motions of twisting and kinking by a hinge. The motions are shown as distinct, but can also be combined. (C) Structural characteristics of KL-L, KL-KL and KL-K. The red color indicate a hydrophobic region and the blue color represents a basic region. (D) Helical wheel diagram of KL-L, KL-KL and KL-K. Red circles refer to hydrophobic residues, blue circles to cationic amino acids.

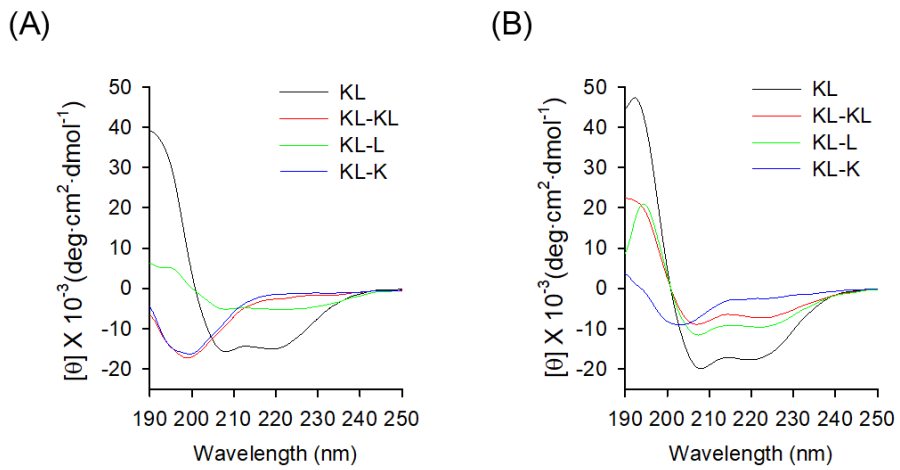


Fig. 2. CD spectra of the peptides. CD spectra were obtained at 25°C in (A) aqueous buffer and (B) 30 mM SDS micelles in the presence of 25 μM of the peptides

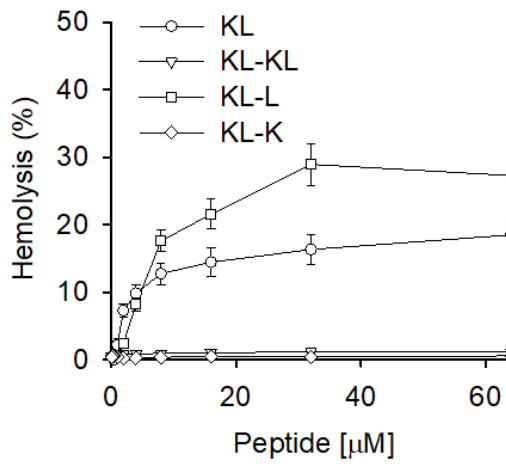


Fig. 3. Dose-dependent curves of hemolytic activity caused by the peptides toward sheep erythrocytes. Assay were carried out as described in the experimental section. Data are shown as mean \pm SD (n = 3).

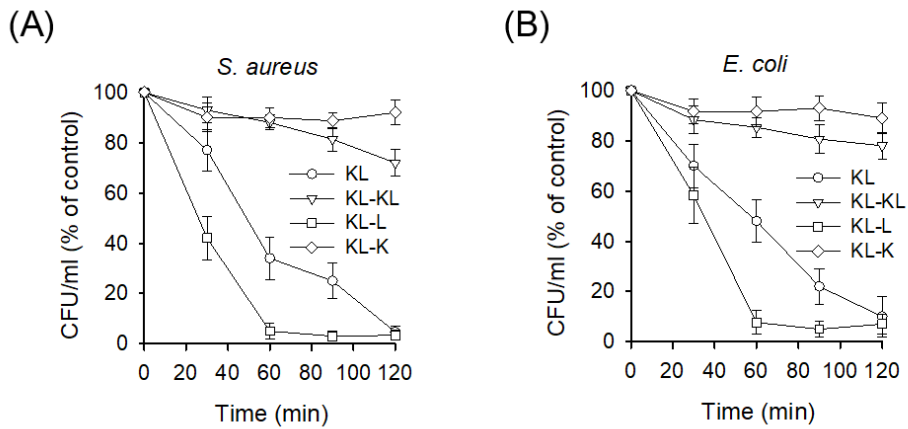


Fig. 4. Killing kinetics of the peptides on bacterial cells. (A) Gram-positive *S. aureus* and (B) gram-negative *E. coli* were exposed to the peptides at 2xMIC and plated on LB agar plates at indicated time points. After 20 h of incubation at 37°C, the colony forming units (CFUs) were enumerated. Data are shown as mean \pm SD (n = 3).

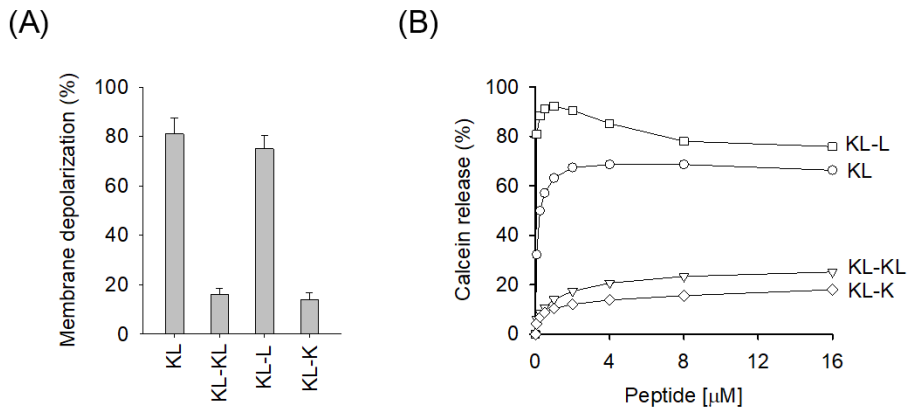


Fig. 5. Membrane permeabilization caused by the peptides (A) Peptide-induced membrane depolarization of *S. aureus*. Complete depolarization was induced by adding Gramicidin D. (B) Membrane disruption induced by peptides. Peptide-induced membrane disruption is defined as the percent calcein leakage from PC/PG (1:1) at a peptide/lipid ratio of 1:20.

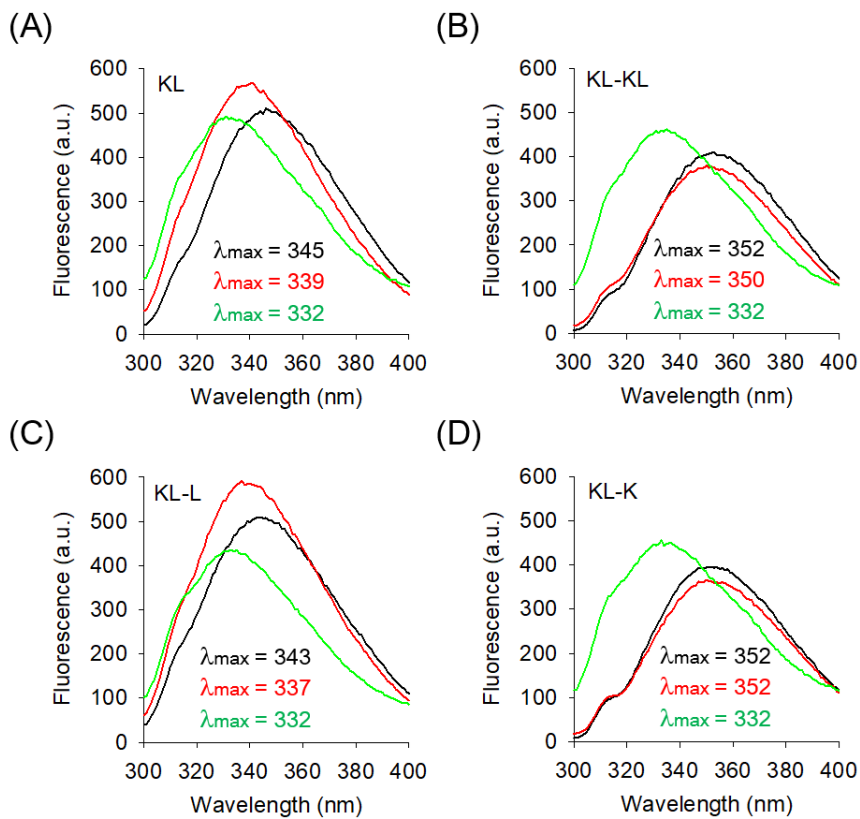


Fig. 6 Tryptophan fluorescence spectra and emission maxima (λ_{max}) for the peptides in buffer (black) and in the presence of vesicles composed of PC/PG (green), or PC (red) at a peptide/lipid molar ratio of 1:100.

References

1. E. F. Haney, S. K. Straus, R. E. W. Hancock, Reassessing the Host Defense Peptide Landscape. *Front Chem* **7**, 43 (2019).
2. A. L. Hilchie, K. Wuerth, R. E. Hancock, Immune modulation by multifaceted cationic host defense (antimicrobial) peptides. *Nat Chem Biol* **9**, 761 (Dec, 2013).
3. L. J. Zhang, R. L. Gallo, Antimicrobial peptides. *Curr Biol* **26**, R14 (Jan 11, 2016).
4. A. Pfalzgraff, K. Brandenburg, G. Weindl, Antimicrobial Peptides and Their Therapeutic Potential for Bacterial Skin Infections and Wounds. *Front Pharmacol* **9**, (Mar 28, 2018).
5. M. Mahlapuu, J. Hakansson, L. Ringstad, C. Bjorn, Antimicrobial Peptides: An Emerging Category of Therapeutic Agents. *Front Cell Infect Microbiol* **6**, 194 (2016).
6. K. Lohner, Membrane-active Antimicrobial Peptides as Template Structures for Novel Antibiotic Agents. *Curr Top Med Chem*, (Jul 13, 2016).
7. L. S. Biswaro, M. G. da Costa Sousa, T. M. B. Rezende, S. C. Dias, O. L. Franco, Antimicrobial Peptides and Nanotechnology, Recent Advances and Challenges. *Front Microbiol* **9**, 855 (2018).
8. A. de Breij *et al.*, The antimicrobial peptide SAAP-148 combats drug-resistant bacteria and biofilms. *Sci Transl Med* **10**, (Jan 10, 2018).
9. P. Kumar, J. N. Kizhakkedathu, S. K. Straus, Antimicrobial Peptides: Diversity, Mechanism of Action and Strategies to Improve the Activity and Biocompatibility In Vivo. *Biomolecules* **8**, (Jan 19, 2018).
10. K. Browne *et al.*, A New Era of Antibiotics: The Clinical Potential of Antimicrobial Peptides. *Int J Mol Sci* **21**, (Oct, 2020).
11. T. A. Stone *et al.*, Positive Charge Patterning and Hydrophobicity of Membrane-Active Antimicrobial Peptides as Determinants of Activity, Toxicity, and Pharmacokinetic Stability. *J Med Chem*, (Jul 1, 2019).
12. S. Guha, J. Ghimire, E. Wu, W. C. Wimley, Mechanistic Landscape of Membrane-Permeabilizing Peptides. *Chem Rev*, (Jan 9, 2019).
13. M. A. Sani, F. Separovic, How Membrane-Active Peptides Get into Lipid Membranes. *Acc Chem Res* **49**, 1130 (Jun 21, 2016).
14. K. Matsuzaki, Membrane Permeabilization Mechanisms. *Adv Exp Med Biol* **1117**, 9 (2019).
15. A. Hollmann, M. Martinez, P. Maturana, L. C. Semorile, P. C. Maffia, Antimicrobial Peptides: Interaction With Model and Biological Membranes and Synergism With Chemical Antibiotics. *Front Chem* **6**, 204 (2018).
16. S. T. Yang, S. Y. Shin, S. H. Shin, The Central PXXP Motif Is Crucial for PMAP-23 Translocation across the Lipid Bilayer. *Int J Mol Sci* **22**, (Sep, 2021).
17. M. N. Melo, R. Ferre, M. A. Castanho, Antimicrobial peptides: linking partition, activity and high membrane-bound concentrations. *Nat Rev Microbiol* **7**, 245 (Mar, 2009).
18. S. B. T. A. Amos *et al.*, Antimicrobial Peptide Potency is Facilitated by Greater Conformational Flexibility when Binding to Gram-negative Bacterial Inner Membranes. *Scientific Reports* **6**, (Nov 22, 2016).
19. S. Q. Li *et al.*, The structure-mechanism relationship and mode of actions of

- antimicrobial peptides: A review. *Trends Food Sci Tech* **109**, 103 (Mar, 2021).
20. Y. Lu, J. Bai, D. Tan, T. Chen, A. Shan, [The effects of hinge structure on the biological activity of antimicrobial peptides and its application in molecular design: a review]. *Sheng Wu Gong Cheng Xue Bao* **37**, 3142 (Sep 25, 2021).
 21. S. T. Yang *et al.*, Possible role of a PXXP central hinge in the antibacterial activity and membrane interaction of PMAP-23, a member of cathelicidin family. *Biochemistry* **45**, 1775 (Feb 14, 2006).
 22. S. Yang *et al.*, Structural analysis and mode of action of BMAP-27, a cathelicidin-derived antimicrobial peptide. *Peptides* **118**, 170106 (Aug, 2019).
 23. S. T. Yang *et al.*, Possible role of a PXXP central hinge in the antibacterial activity and membrane interaction of PMAP-23, a member of cathelicidin family. *Biochemistry* **45**, 1775 (Feb 14, 2006).
 24. H. J. Shin, S. Yang, Y. Lim, Antibiotic susceptibility of Staphylococcus aureus with different degrees of biofilm formation. *J Anal Sci Technol* **12**, (Sep 24, 2021).
 25. H. Lee, S. Yang, S. Y. Shin, Improved Cell Selectivity of Symmetric alpha-Helical Peptides Derived From Trp-Rich Antimicrobial Peptides. *B Korean Chem Soc* **41**, 930 (Sep, 2020).
 26. S. T. Yang, S. Y. Shin, K. S. Hahm, J. I. Kim, Different modes in antibiotic action of tritrypticin analogs, cathelicidin-derived Trp-rich and Pro/Arg-rich peptides. *Biochim Biophys Acta* **1758**, 1580 (Oct, 2006).
 27. L. Zhang, P. Dhillon, H. Yan, S. Farmer, R. E. Hancock, Interactions of bacterial cationic peptide antibiotics with outer and cytoplasmic membranes of Pseudomonas aeruginosa. *Antimicrob Agents Chemother* **44**, 3317 (Dec, 2000).
 28. S. T. Yang *et al.*, Contribution of a central proline in model amphipathic alpha-helical peptides to self-association, interaction with phospholipids, and antimicrobial mode of action. *FEBS J* **273**, 4040 (Sep, 2006).
 29. S. T. Yang *et al.*, Contribution of a central proline in model amphipathic alpha-helical peptides to self-association, interaction with phospholipids, and antimicrobial mode of action. *Febs J* **273**, 4040 (Sep, 2006).
 30. J. K. Boparai, P. K. Sharma, Mini Review on Antimicrobial Peptides, Sources, Mechanism and Recent Applications. *Protein Pept Lett* **27**, 4 (2020).
 31. N. Mookherjee, M. A. Anderson, H. P. Haagsman, D. J. Davidson, Antimicrobial host defence peptides: functions and clinical potential. *Nature Reviews Drug Discovery* **19**, 311 (May, 2020).
 32. S. Nayab *et al.*, A Review of Antimicrobial Peptides: Its Function, Mode of Action and Therapeutic Potential. *Int J Pept Res Ther* **28**, (Jan, 2022).
 33. Y. X. Lin *et al.*, Study on the Structure-Activity Relationship of an Antimicrobial Peptide, Brevinin-2GUb, from the Skin Secretion of Hylarana guentheri. *Antibiotics-Basel* **10**, (Aug, 2021).
 34. C. F. Le, C. M. Fang, S. D. Sekaran, Intracellular Targeting Mechanisms by Antimicrobial Peptides. *Antimicrob Agents Chemother* **61**, (Apr, 2017).